UPPSALA
UNIVERSITET

UPTEC X 16 024
Examensarbete 30 hp
Juli 2016

Single-cycle kinetics for QCM biosensors for high throughput nanoparticle characterization application

Fredrik Boström

UPPSALA UNIVERSITET

Degree Project in Molecular Biotechnology

Masters Programme in Molecular Biotechnology Engineering,
Uppsala University School of Engineering

UPTEC X 16 024	**Date of issue 2016-07**

Author

Fredrik Boström

Title

Single-cycle kinetics for QCM biosensors for high throughput nanoparticle characterization application.

Abstract

Characterizing nanoparticles to be able to understand how they functions in the body is important for development of drugs. Furthermore with increasing number of nanoparticle product the nanotoxicity of nanoparticles is important to understand. This report is a part of the EU-project Nanoclassifier which purpose is to "develop a cost effective, high throughput screening platform for characterization of the bionanointerface and its cell-binding partners". Single-cycle kinetic was used to determine the number of binding epitopes on polystyrene nanoparticle with transferrin corona. The number of available epitopes describes how active the Nanoparticle will be in the body. For this purpose Single-cycle kinetic methodology was successfully used on nanoparticles. Single-cycle kinetic methodology has great potential to become the standard method for high throughput nanoparticle epitope characterization.

Keywords

Single-cycle kinetics, nanoparticles, QCM, biosensor, kinetics, image analysis, cell counting

Supervisors

Samuel Altun
Attana

Scientific reviewer

Helena Danielson
Uppsala University

Project name -	Sponsors -
Language **English**	Security -
ISSN 1401-2138	Classification -
Supplementary bibliographical information	Pages **56**

Biology Education Centre Biomedical Center Husargatan 3, Uppsala
Box 592, S-751 24 Uppsala Tel +46 (0)18 4710000 Fax +46 (0)18 471 4687

Single-cycle kinetics for QCM biosensors for high throughput nanoparticle characterization application

Fredrik Boström

Populärvetenskaplig sammanfattning

Intresset för nanopartiklar har ökat det senaste årtiondet. Möjligheten att använda nanopartiklar i olika mediciner mot t.ex. cancer har hög potential. Dessutom så ökar antalet produkter som innehåller nanopartiklar varje år. För att säkerställa snabb och säker utveckling av nanopartiklar så måste man kunna karaktärsira nanopartiklar snabbt och kostnadseffektivt. Den här rapporten föreslår en metod att karaktärisera nanopartiklar med biosensorer.

När nanopartiklar åker in i kroppen så fastnar det proteiner på nanopartikeln. Det är inte nanopartikeln utan det proteinlager på nanopartiklen som interagerar med omgivningen. Därför är det väldigt viktigt att undersöka detta proteinlager eftersom det är proteinlagret som styr nanopartikelns öde i kroppen.

Det här examensarbetet syftar till att utveckla effektiva metoder för att analysera nanopartiklar. I denna rapport används biosensorer för att undersöka hur en nanopartikel interagerar med celler. För detta har alternativ metod för att mäta kinetik testats på biosensorer av kvartskristall. Denna metod är snabbare och kan analyser en större variation av interaktion än den vanliga metoden.

En bildanalysmetod har utvecklats för att mäta hur mycket som binder på en cell. Till detta har ett program använts för att analysera chip med bundna celler. Syftet är att utveckla en metod för att räkna celler på detta chip.

Detta projekt är en del av ett större EU projekt vilkets syfte är att ta fram en snabb och kostnadseffektiv metod för att analysera nanopartiklar. Denna rapport föreslår en sådan metod och applicerar den på nanopartiklar.

Examensarbete 30 hp
Civilingenjörsprogrammet Molekylär bioteknik
Uppsala universitet, juli 2016

List of Contents

List of abbreviations and acronyms

ab_XXX	Antibody xxx
ANOVA	Analysis of variance
CV	Coefficient of variation
B_{max}	Maximum response
D_{max}	The maximum cell diameter
D_{min}	The minimum cell diameter
k_a	Association rate constant
k_d	Dissociation rate constant
K_D	Dissociation equilibrium constant
MCK	Multi-cycle kinetics
NP100	Polystyrene nanoparticle with diameter 100 nm
NP200	Polystyrene nanoparticle with diameter 200 nm
NPXXX@Tf	XXX nm diameter polystyrene particle with transferrin corona
QCM	Quartz crystal microbalance
SCK	Single-cycle kinetics
Tf	Transferrin
TfR	Transferrin receptor

1 Introduction

Understanding how nanoparticles function and the application of nanoparticles is of growing interest. Nanoparticles as medicine or drug delivery system for cancer treatment has great potential. Nanoparticles containing anti-cancer component can target cancer cells and increase the concentration of the anti-cancer drug. Furthermore, nanoparticles could enter the cell by endocytosis resulting in drug delivery directly into the cells [1], [2]. It is therefore important to understand and characterize nanoparticles to enable faster research in the field.

Nanotoxicity is an emerging field which purpose is to better understand "the potential toxic impact of nanoparticles on biological and ecological systems" [3]. The number of products containing nanoparticles is increasing and to better understand their impact on health is therefore very important [3]. This is important for development of safe nanomaterials.

This project is a part of the EU project: Nanoclassifier. The Nanoclassifier project is a collaboration between Center of Bionanointeraction at university college Dublin and Attana. The purpose of the project is to develop a high throughput and cost effective method to characterize nanoparticles using Attana's quartz crystal microbalance (QCM) biosensors [4]. This report purpose is also to enable epitope mapping on a nanoparticle corona using QCM biosensors and affirm the result from an article produced by Center of Bionanointeraction.

Due to difficulty to perform kinetic evaluation of nanoparticles, a protocol for single cycle kinetic experiment has been developed for Attana's instrument. Single-cycle kinetic (SCK) experiments is a different way to perform kinetic experiment, compare to multi cycle kinetic experiments which is a standard procedure [5]. The SCK protocol can be applied to characterize nanoparticles but can also be applied to other interactions, making it a very valuable method for Attana.

Assay development has also been done by enabling the counting of cells on the Attana's chip using the free image analyzing software Cellprofiler. This enables Attana to determine the number of cells on the sensor surface and this can also be applied to the Nanoclassifier project determination of the number of nanoparticles bound per cell.

In this report I propose a high throughput method to characterize nanoparticles using QCM biosensors. This is in line with the Nanoclassifier project which aim is to determine a cost effective and high throughput method to characterize nanoparticles [4]. Nanoparticles could be the drug of the future and the methods described in this report can lead to a standardized method for evaluating nanoparticles.

1.1 Background

1.1.1 Aim and scope

The aim of this master thesis project is to develop methods for high throughput nanoparticle characterization. This project is a part of the EU project Nanoclassifier which is a collaboration between Attana and the center of BioNanointeraction from the University College Dublin (UCD). The purpose of the Nanoclassifier project is to "develop a cost effective, high throughput screening platform for characterization of the bionanointerface and its cell-binding partners" [4]. For this purpose SCK methodology is used on Attana's QCM biosensors. The SCK methodology is applied on 100 nm polystyrene nanoparticle to identify number of binding epitopes.

The project initially was involving measuring binding on cells, a method for counting cells on the chip has been developed. This method would make it possible to determine the amount of nanoparticles bound to each cell.

1.1.2 Nanoparticles

When nanoparticles come in contact with a biological medium such as blood or other fluids, a protein corona is formed around the nanoparticle [2], [6], [7]. Depending on the shape, size, charge and functionalization of the nanoparticle different coronas will form [2], [6]. Furthermore, the protein composition of the corona depends on the composition of the biological medium [6]. It's not the nanoparticle, but the protein corona that will interact with its surroundings. For example, if the nanoparticle has a protein corona constituting of transferrin, the nanoparticle would interact with transferrin receptors in the body. The protein corona will therefore be the bio-interface of the particle and determine its fate in the body [6].

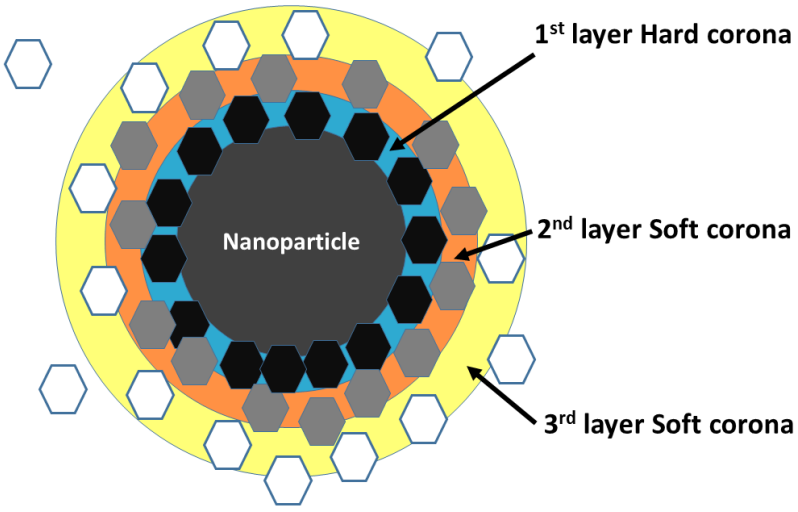

Figure 1. **Schematic picture of the different coronas on a nanoparticle submerge in a biological medium consisting of a single protein.** The first layer is called hard corona and has the most strongly bound proteins seen as black hexagons. The second layer is less tightly bound and is therefore a soft corona (grey hexagons) and the third layer is very loosely bound (white hexagons).

There are two different types of coronas: hard corona and soft corona. Protein bound in the first layer is almost irreversibly bound to the nanoparticle, forming a hard corona (Figure 1). The hard corona is hypothesized to bind to the nanoparticle by lowering the surface free energy of the nanoparticle surface. The hard corona is stable for hours and can therefore be used in experiment. The soft corona forms secondary or tertiary layers above the hard corona. The proteins forming the soft corona doesn't bind directly to the surface and weaker forces is holding the soft corona in place. Exchange of proteins takes place, proteins with higher affinity to the surface can replace proteins in the corona. If the nanoparticle containing a soft corona is exposed to a variety of proteins, it's very likely that the composition of the soft corona will change [7]. The exchange rate is in the minute timeframe for the soft corona and therefore changes very rapidly when exposed to different proteins. This project uses transferrin as the protein corona.

A big part in characterizing nanoparticle is to determine how many exposed epitopes there are on the protein corona. When transferrin attaches to the surface, the orientation is random. This makes the exposed epitopes, which a receptor or antibody can attach to, also random. Determining binding epitope is to verify result from an article by Kelly et al., (2015). In the article they use different imagine techniques to identify the number of anti-transferrin antibody binding spots, while in this report SCK is used to determine the number of binding epitopes on the nanoparticles [8]. The number of binding epitopes is important to know because it describes how active the nanoparticle will be in the body and potential drug applications.

1.1.2.1 Transferrin

In this project transferrin is used to produce the protein corona around the nanoparticles that constitutes the bio interface. Transferrin is the main iron transporting protein in humans. Transferrin is 80 kDa, homodimer that binds ferric and ferrous iron and transport it around the body. Transferrin is a homodimer and binds two iron at a pH 7.4 which is the extracellular pH. When the transferrin bind two iron, conformation change occur which make it able to bind to the transferrin receptor (TfR). The TfR can bind two transferrin and when transferee the signal which endocytoses the transferrin. The inside of the vacuole is then acidified which changes the pH and releases the iron from the transferrin. The vacuole is then merged with the cell membrane which releases the transferrin so it can bind more iron and continue the cycle [9].

The transferrin cycle is of interest in cancer drug targeting. Cancer cells require large quantities of iron to grow and spread in the body. The cancer cells overexpresses TfR to acquire enough iron [10]. A nanoparticle can therefore enter the cells and deliver the drug inside the cell. This makes TfR a good target for cancer drugs because the drug will accumulate around the cancer, sparing other parts of the body that might get affected with other unspecific cancer drugs.

1.1.3 Single-cycle kinetics

Multiple- cycle kinetic (MCK) is the normal method to perform kinetic experiments. MCK is performed by injecting different concentrations of analyte over the sensor surface and regenerate the surface after each injection to clear the sensor surface from analyte [5]. This is done for several concentrations. MCK is the most common way to perform kinetic evaluation and ensures precise measurements. Single cycle kinetics (SCK) or kinetic titration as it is also called, is another method to perform kinetic evaluation experiments. SCK is performed by multiple

injections of analyte in a single run, in increasing concentrations without regenerating the surface. There is no regeneration between injections making it optimal for surfaces where regeneration is difficult or impossible [5]. The resulting kinetic data is very similar to multi-cycle kinetics [12].

When regenerating, the ligand is exposed to extreme conditions to sever the bond of ligand-analyte. This is normally done by lowering or increasing the pH and it can affect the ligand in such a way that it loses its binding capabilities [5]. SCK can be used to avoid decreasing of the surface activity [12]. There are also cases when regeneration is impossible, the bond between ligand and analyte is too strong to break. Then MCK is impossible and SCK is the only choice.

To plan an optimal SCK experiment you need to make preliminary experiments to determine the optimal concentrations to get accurate results [13]. In an article by Palau and Di Primo (2013) the author propose a preliminary experiment and simulations to improve experimental design of SCK experiments. In the article they describe a three step process. First perform a single concentration with regeneration. Then use the kinetic data from the single concentration experiment for simulations. When analyzing the simulations, the optimal concentration and dilution factors can be determined and the SCK experiment is then performed with the determined concentrations. This assures that the SCK experiment produces accurate data.

To verify that SCK works on the Attana A200 machine SCK and MCK experiment with myoglobin and anti-myoglobin antibody are performed on the same chip. This is done on three different chips on the same machine. The aim of these experiment is to validate that you can achieve the same data with SCK experiment as with MCK experiment. It's important to note that the type of interaction is not important, only that the same information is produced from the different methods. Statistical analysis of the data is performed to verify this.

1.1.3.1 Myoglobin

Myoglobin and anti-myoglobin (ab_7005) is the model system used at Attana for biochemical educational purposes. The interaction system is well characterized and makes it an optimal system for verifying SCK. Myoglobin is oxygen carrying protein and transports oxygen to the mitochondria by reversely binding oxygen. Myoglobin also facilitates oxygen storage and high levels of myoglobin can be found in diving mammals [14].

1.1.4 Cell counting

Image analysis is important in various fields of science. There are several traits that can be determined by manually analyzing images. The process needs an experienced eye and the process can be labor intensive. With increasing computing power and advances in programming, automatic image analysis tools can be used. In contrast to manually analyzing images, a program can take in consideration more parameters and analyze more quantitative. A program can also be more comparable analysis because it does not rely on experience. With the right staining, a program can for example detect changes in DNA quantities and detect phenotype in variation of cell size [15]. In this report the image analyzing software CellProfiler is used to count cells.

CellProfiler is an open source software for image analysis and uses a modular system which enables complex image analysis that can be performed by individuals with no programming

experience [15]. The researcher sets up a "pipeline" containing "modules" that perform analysis or modification of the image. This enables fast set up for different experiments. When the pipeline is set up it can easily be shared and modified to fit the equipment of a customer or project. The result can also be comparative, which enable Attana to set a defined standard for confluence and make experiments more comparable in Attana's cell based assays.

The variable that affect cell count in the "IdentifyPrimaryObjects" module the most is D_{min}. D_{min} and D_{max} is set as the typical diameter of an object. D_{min} determine how small an object can be. Objects in this case is cell nuclei which has been stained and a image taken using a microscope. It's therefore important to know the lowest size of a nuclei to get an accurate cell count. If D_{min} is set too low, then Cellprofiler will identify too many objects that are not nuclei. If the D_{min} is set too high CellProfiler will exclude objects which are nuclei. D_{max} only effect the cell count if it set too low and is therefore set very high to not exclude objects. The sensor surface only contains cells and groups of cells which can be distinguished even with a high D_{max}. There are various things that determine the diameter of a nuclei in an image. For example the zoom will change the size of the nuclei in the image. Several biological factor can also determine the size of the nuclei. Therefore it's important to determine the D_{min} for at least each microscope and cell line. The pipeline "DminAnalyzer" was setup to determine D_{min} easily.

$$n_{images} = \frac{S_{chip}}{N_{bacterial\ total}\varepsilon S_{image}} \qquad \text{(Equation 1)}$$

Equation 1 is taken from an article by Tsougeni *et al.* (2016) [16]. In the article the authors use a program to automatically count the number of bacteria on their chip. This equation is an indication on how many images that needs to be taken to get an accurate number of the cells on the chip. n_{images} is the number of images that needs to be taken to get an accurate cell count of the surface. S_{chip} is the area of the chip and S_{image} is the area of the image. $N_{bacterial\ total}$ is the concentration of cells that you put on your surface. ε is the relative error.

File format is very important when analyzing images. In this report JPEG images are analyzed because the images used where taken from previous projects. JPEG is not recommended for use because it creates artifacts [17]. The recommended file formats is bmp, gif, png or tif [15], [17]. These formats doesn't lose information and are better suited for image analysis.

Two image analysis experiments is performed. Two images of fixated cells is analyzed. The two images is from two different chips. Lastly four images of the same chip is analyzed. The cells are not adherent. All of the experiments are performed in 3 steps. First is cell count for each D_{min} determined. Then the image or a part of the image manually counted for reference. With this data an accurate D_{min} is determined and the automatic cell count of the whole image is performed.

Automatic analyzing images can result in an accurate cell count on the chip surface. This number is valuable when comparing between chip and for further research. With the relative simple method valuable data can be extracted. Further investigation can also result in a more accurate standardization of confluence which in the past has been evaluated by eye. This would increase

the reproducibility between chips. This report enables improvement of the Attana cell based assay.

2 Method

2.1 SCK

2.1.1 Experimental setup

Attana's A200 machine were used to perform these experiment. Anti-myoglobin (ab_7005) were immobilized on Attana's LNB chip using standard amine coupling.

To perform the immobilization, the running buffer was 1x HBST (10mM HEPES, 150 mM NaCl and 0.005% Tween) at a 10 µl/min flowrate. 0.4 M EDC and 0.1M sNHS were mixed 1:1 and injected over the chip surface for 300s in both channel A and channel B. The Anti-myoglobin antibody (ab_7005) was diluted to 5 µg/ml and injected over channel A for 300s. The surfaces were then deactivated with an injection of ethanolamine 1 M for 300s over both channel A and channel B. The resulting immobilizations of all three chips can be seen in Figure 7.

The kinetic experiments were performed in 22 °C with 25 µl/min flow rate. The running buffer used was 1x HBST (10mM HEPES, 150 mM NaCl and 0.005% Tween). The regeneration was performed with 10mM Glycine pH 2.5.

Myoglobin was diluted to 2 µg/ml in HBS-T buffer and was used to perform a single injection. The resulting initial experiment for chip 2.2 can be seen in Figure 8. The association phase was set to 84 s and the dissociation was 300 s followed by regeneration with 10 mM Glycine pH 2.5. The kinetic evaluation was done in ClampXP using a 1:1 model and the kinetic data was used to determine optimal concentration for the SCK and MCK experiment. The simulations for optimal concentrations can be seen in Figure 9. How to perform a simulation is described in section 2.1.3.

A 2-fold dilution series was prepared resulting in concentrations of 2, 1, 0.5, 0.25 and 0.125 µg/ml for the chip 2.2 and chip 2.3. The concentrations for chip 2.4 were 1, 0.5, 0.25, 0.125 and 0.0625 g/ml. The machine was programmed using C-fast software and the resulting programming list for SCK and MCK experiment can be seen in Appendix 3. The SCK run was performed 84 s association, 168 s dissociation and the last dissociation time set to 600 s. Figure 10 shows the resulting SCK experimental data. Curve fitting was done using ClampXP and the parameters from the initial single run were used as initial parameters for SCK fitting. The curves were fitted with a 1:1 binding model.

MCK experiment was performed on the same chip for reference. The result of MCK experiment can be seen in Figure 12. The concentrations is the same as in the SCK experiment. The association time is 84 s,the dissociation time is 300 s and the regeneration performed by injection of 10 mM Glycine pH 2.5. The C-fast program for both SCK and MCK can be seen in Appendix 3.

The experiment was performed three times on three different chips. The kinetic parameters were determined by using Attana's evaluation software to extract the curves and the program ClampXP to determine the kinetic constants. The kinetic parameters was statistically analyzed using Excel.

2.1.2 Analyzation

2.1.2.1 SCK curve fitting

This section shows how to evaluate kinetic data from SCK experiments using the software ClampXP.

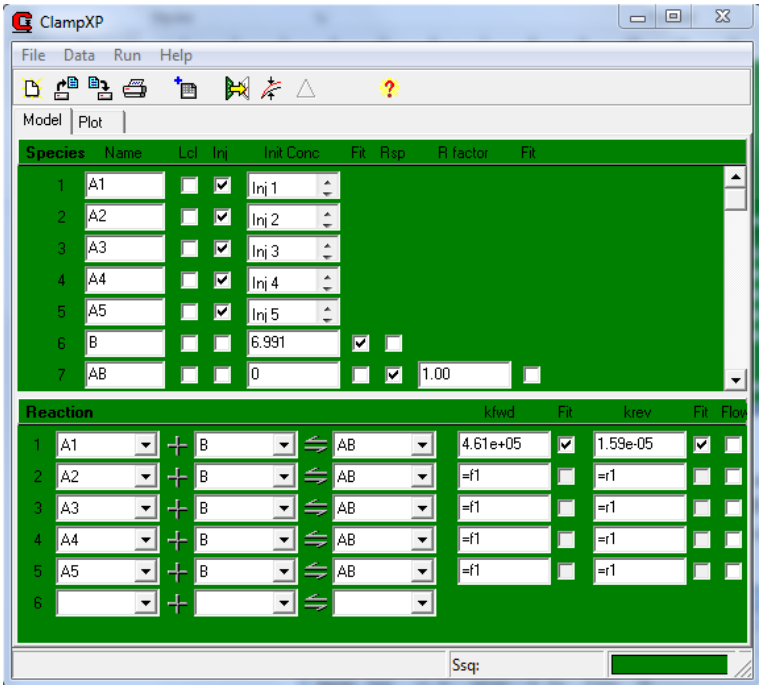

Figure 2. **The model page in ClampXP for SCK experiment analysis for 1:1 binding model.** Each injection is a separate reaction with same rate constants are used for fitting.

Figure 2 show how to set up the model page to simulate SCK data. Each concentration is a separate injection. In the lower half of the page is where the reactions is described. Each injection has the same kinetic parameters indicated by =f1 and =r1. The association constant (k_a), dissociation constant (k_d) and maximum response (B_{max}) parameter is all parameters included in the curve fitting.

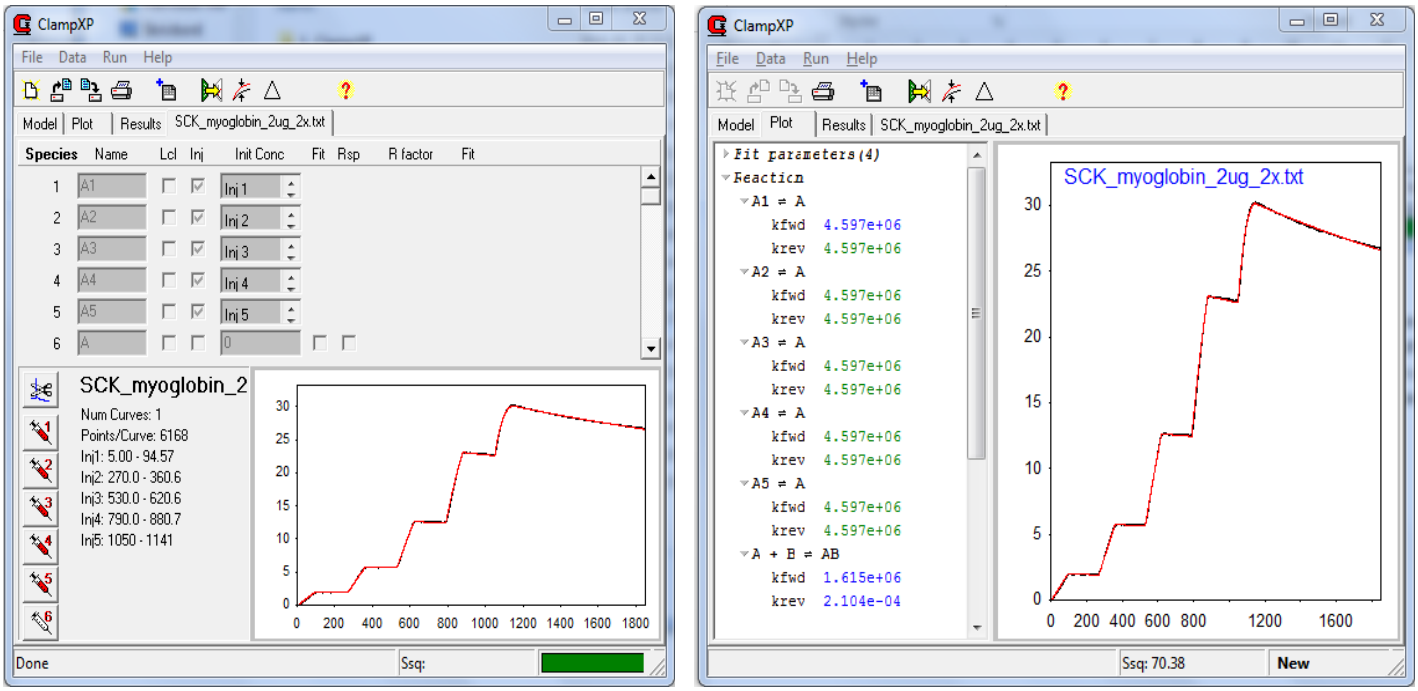

Figure 3. **The data page and plot window in ClampXP.** Data page can be seen to the left. The injection time and concentrations can be set by pressing the syringes. Spikes can be cut by pressing the scissor button. The plot page can be seen to the right. By pressing simulated, a simulated curve is produced with the initial parameters in the model page. Pressing the fit button fits the data to the curve. The kinetic constants can be seen under reaction.

The data page is where the raw data from the run is imported (Figure 3). The injection time and concentration need to be set for each concentration. Curve spikes can be cut by pressing the "scissor" button. After the injection time is set, ClampXP can simulate the curve with the initial parameters. Then curve fitting can be done and the resulting kinetic parameters can be seen in the left window.

2.1.2.2 Statistical evaluation

A T-test was performed on the kinetic data. The k_a, k_d and K_D was compared between the SCK and MCK. The null hypothesis was tested for all the sets. The analysis was performed in excel. The T-test settings were paired and a two side distribution.

An Analysis of Variance (ANOVA) analysis was performed on the data sets. The ANOVA analysis was performed in excel using the two-factor with replication model.

2.1.3 Curve simulation

6 data pages were loaded with curves containing only zeros. The association time was set to 84 s and dissociation time was set to 168 s for all data pages. Each data page has different concentrations and different dilution factor. The simulations are done by typing in the kinetic constants in the model page (Figure 2) and simulate. The resulting plot page will look as in Figure 9.

2.2 SCK Nanoparticles sandwich assay

Anti-transferrin (ab_769) were immobilized on Attana's LNB chip using standard amine coupling. The running buffer used were 1x PBS buffer at a 10 µl/min flowrate.

0.4 M EDC and 0.1M sNHS were mixed 1:1 and injected over the chip surface for 300 s in both channel A and Channel B. Anti-transferrin (ab_769) was diluted to 50 µg/ml and injected over channel A for 300 s. The surfaces were then deactivated with an injection of 1 M ethanolamine. The resulting immobilization of anti-transferrin can be seen in Figure 15.

The kinetic experiments were performed in 22 °C and 25 µl/min flow rate. The running buffer used were 1x PBS and the regenerations were performed with 10 mM Glycine pH 2.5.

The nanoparticles was prepared by first measuring 2.5 mg transferrin. The 2.5 mg transferrin was diluted in MES buffer (50 mM, Ph 6) and mixed with 19 µl nanoparticles to a total volume of 500 µl. The mixture was incubated for 1 hour in 37 °C under shaking. The nanoparticles transferrin mixture was centrifuged for 10 min in 15000 rcf for NP100 or 20000 rcf for NP200. The supernatant was removed and the pellet resuspended in fresh MES buffer. This step was repeated 3 times. The tubes was then centrifuged and the pellet resuspended in PBS buffer, repeated 2 times. The prepared nanoparticles lasts 5 day before expiring.

2.2.1 Experimental setup

Table 1. **Kinetic data and affinities from a previous NP100@Tf MCK sandwich assay experiment performed by Maria Gianneli**. The anti-transferrin (ab_769) concentrations used are 60, 40 20 10 and 5 µg/ml. The kinetic constants was determined using Attana's evaluation software.

MCK Kinetic data	
B_{max} (Hz)	4,07
k_a $(M^{-1}s^{-1})$	5,06E+05
k_d (s^{-1})	2,01E-04

To determine the concentration of anti-transferrin (ab_769) analyte, kinetic data from a previous NP100@Tf MCK sandwich assay experiment performed by Maria Gianneli was used. These parameters can be seen in Table 1.

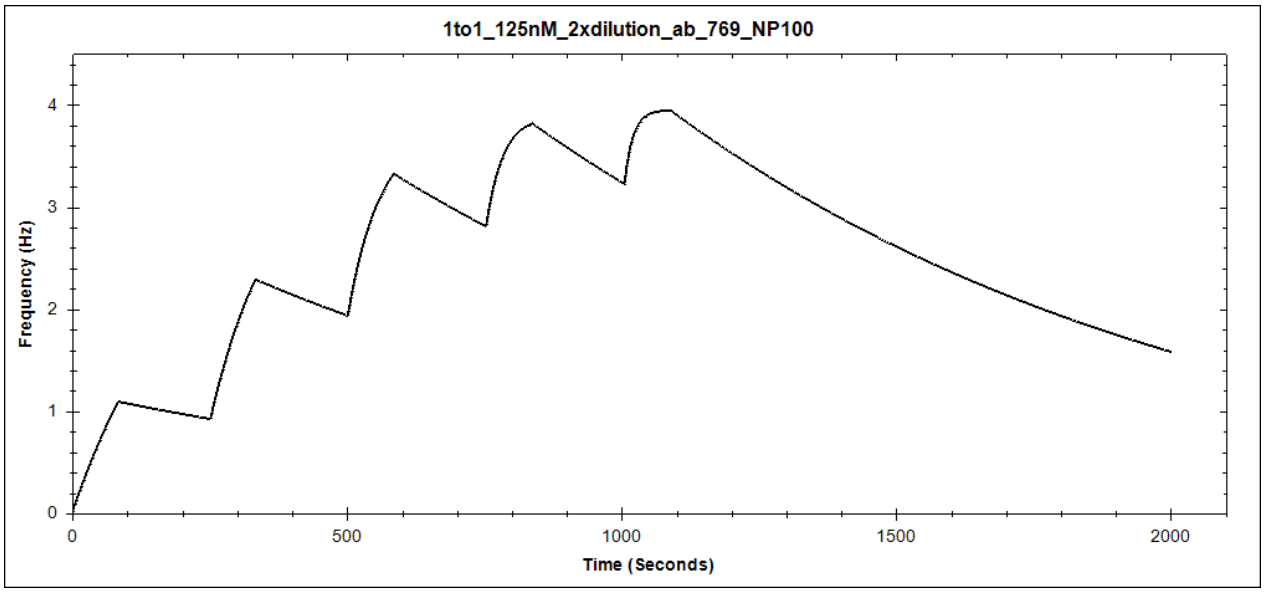

Figure 4. **The sensorgram show the simulated interaction of transferrin and anti-transferrin (ab_769) using the kinetic constants from Table 1.** Simulations was performed using ClampXP with the method described in section 2.1.3. The highest concentration is 125 nM transferrin with 2x dilution factor.

Figure 4 show the chosen simulated curve. The curve clearly reaches B_{max} and saturates the surface. The experiment consists of first attaching NP100@Tf as a second ligand. Then perform a SCK experiment with anti-transferrin (ab_769) as analyte. The C-fast programming list that show the injection steps is shown in Appendix 4.

2.2.2 NP100 concentration determination

To taking into account to difference in concentrations when preparing nanoparticles a concentration experiment was performed. This is done by injecting different concentrations of NP100 to achieve a response of around 20 Hz which is the same response as reference experiment performed by Maria Gianneli.

2.3 Cell counting

2.3.1 Image method

Cells where grown over the course of several weeks according to Attana's "Passing cells" protocol. The cells where seeded overnight and immobilized using Attana's "Stabilization of the cells with glutaraldehyde" protocol. The cells nuclei was stained according to Attana's "DAPI staining of cell nuclei" protocol.

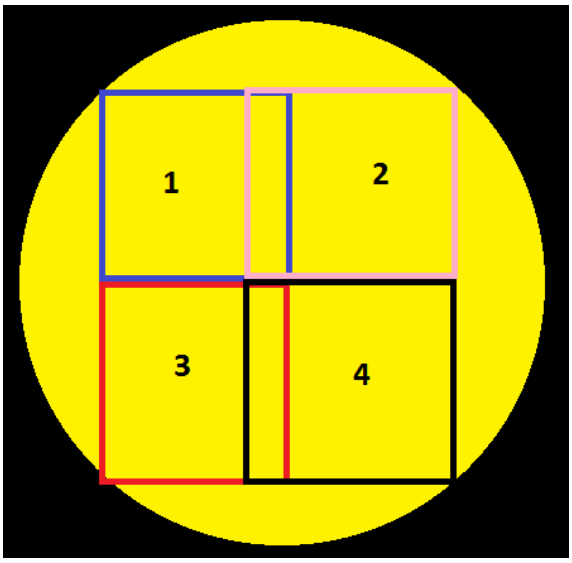

Figure 5. **Schematic image describing how to take images of the chips sensor surface to achieve an accurate cell count**. The yellow circle represents the chip and the squares represents the images. 4 images is taken with the edge of the image in line with the edge of the sensor surface.

After the cells were seeded overnight, 4 were taken with the Nikon eclips 80i microscope on 4X magnification. The position of the image can be seen in Figure 5.

2.3.2 Pipelines setup

To determine an accurate D_{min} a "DminAnalyzer" pipeline was setup with D_{min} ranging from 1-9 pixels. The image was cropped to 200x200 pixel and manually counted. The D_{min} was

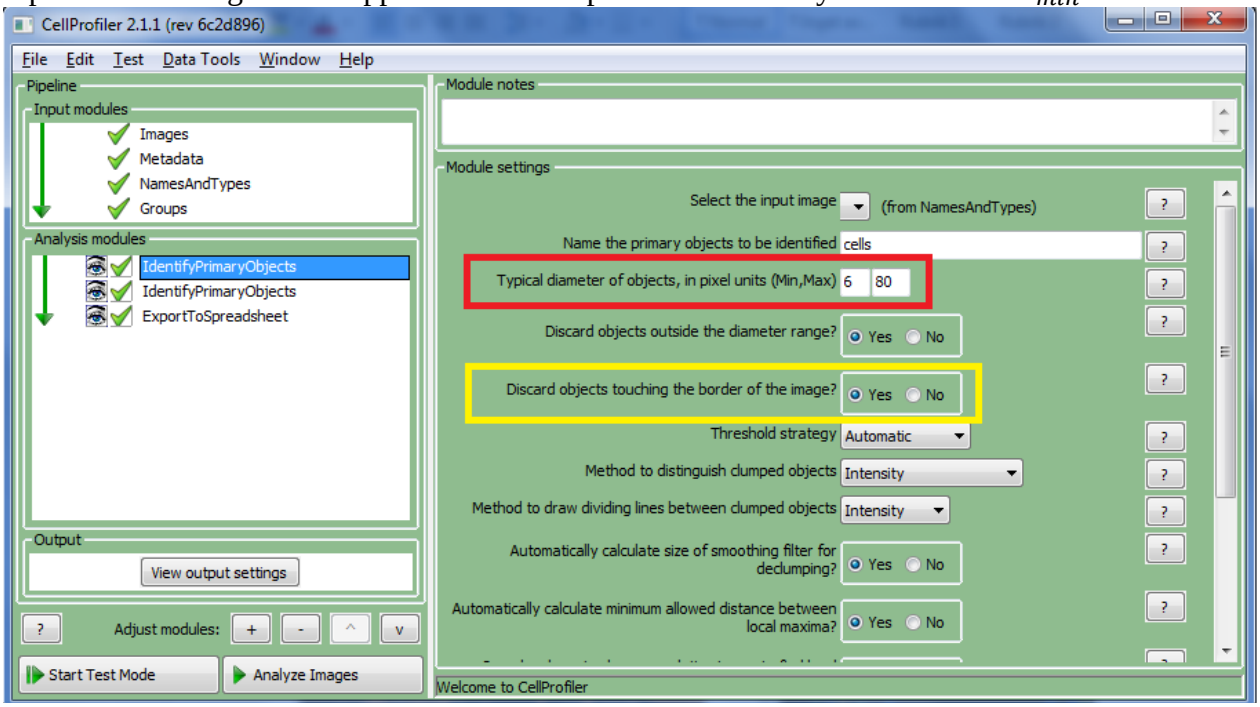

Figure 6. **Configuration of theIdentifyPrimaryObjects module in the CellCounter pipeline**. Both "identifyPrimaryObjects" modules has the same D_{min}. The difference between them is one discards objects touching the sides and one doesn't as sen circled in yellow.

determined by choosing the D_{min} which produced a cell count closest to the manually counted cell number.

The “CellCounter” pipeline was then setup in three steps as seen in Figure 6. The first and second module is “identifyPrimaryObjects” which identify nuclei in the image. The difference between the first and the second “identifyPrimaryObjects” is one discards cell nuclei that is touching the sides. The last module,”ExportToSpreadsheet”, compiles the extra data in a file that can then be evaluated.

2.3.3 Script usage

The data can be manually extracted and calculated from the output files. For this experiment a script “CellCountCompiler” was written in the programming language Python using the IDE free software PyCharm. The script can be seen in Appendix 1 and the output folder location is put in line 7. The name of the output files must contain the word “cell” as can be seen in line 8. The script is then executed and the output is the number of cells from each analysis, mean cells per analysis, area covered by objects (cell nuclei) and the mean area covered by cell nuclei.

2.3.4 Experimental method

Two images taken with the Nikon eclips 80i microscope on 4X magnification of the cells on two different chips was analyzed. The images were analyzed using the “DminAnalyzer” pipeline which cropped the images to 200x200 pixels and counts the cells with different D_{min}. The images were then manually counted and D_{min} determined by comparing the automatically and manually counted numbers. Both images were analyzed with “CellCount” pipeline and a cell number of the image was determined.

To determine an accurate cell count on a single chip, four images were taken according to the setup shown in Figure 5. The cells were not fixated to the surface. The top left of the four images were used to determine the D_{min} (Figure 23). The image was cropped in the lower right corner and analyzed with “DminAnalyzer” pipeline. The cropped image was also manually counted. The D_{min} was determined to 3 pixels by comparing the manually counted number to the closest cell count for the D_{min}. All of the four images were then put through the “CellCounter” pipeline D_{min} set to 3 and the result was compiled using the “CellCountCompiler” script.

3 Result

3.1 SCK

3.1.1 Immobilization

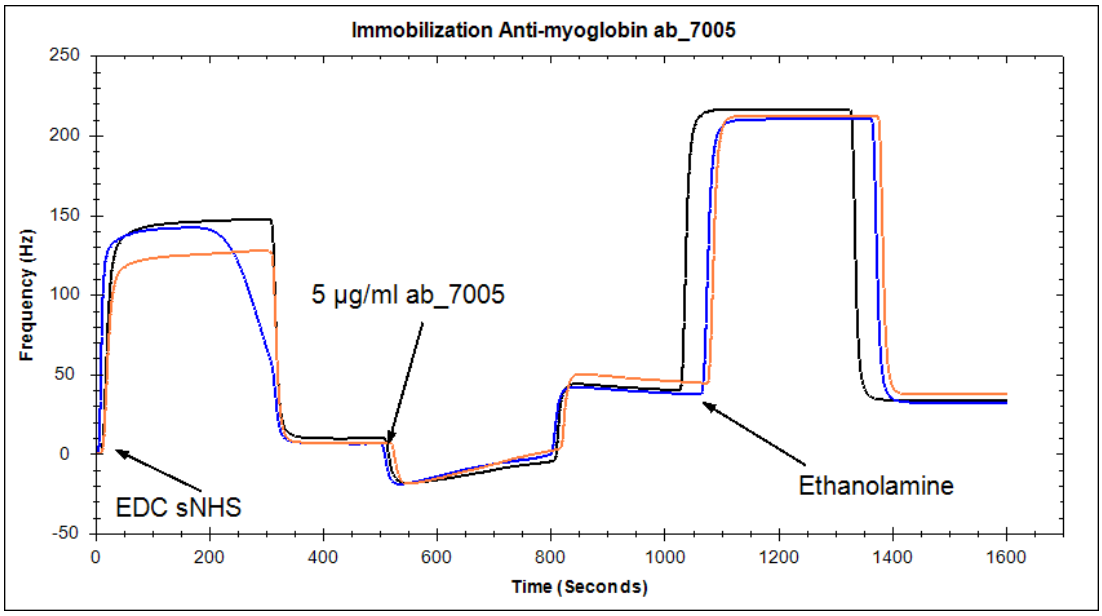

Figure 7. **Sensorgrams of the immobilization Anti-myoglobin antibody (ab_7005) on three chips.** Fist an injection of EDC and sNHS mixture was injected for 300s. Then 5 µg/ml anti-myoglobin was injected for 300 s. The surface was then deactivated by injecting ethanolamine for 300s.

Figure 7 show the immobilization of 5 µg/ml ant-myoglobin (ab_7005) with amine coupling. The immobilized mass corresponds to 30 Hz. The three different chips used is called chip 2.2, chip 2.3 and chip 2.4. Chip 2.3 and chip 2.4 achieve a lower immobilization than Chip 2.2. All immobilizations is very similar to each other. This surface density is lower than previously tested to counteract mass transport.

3.1.2 Experimental design

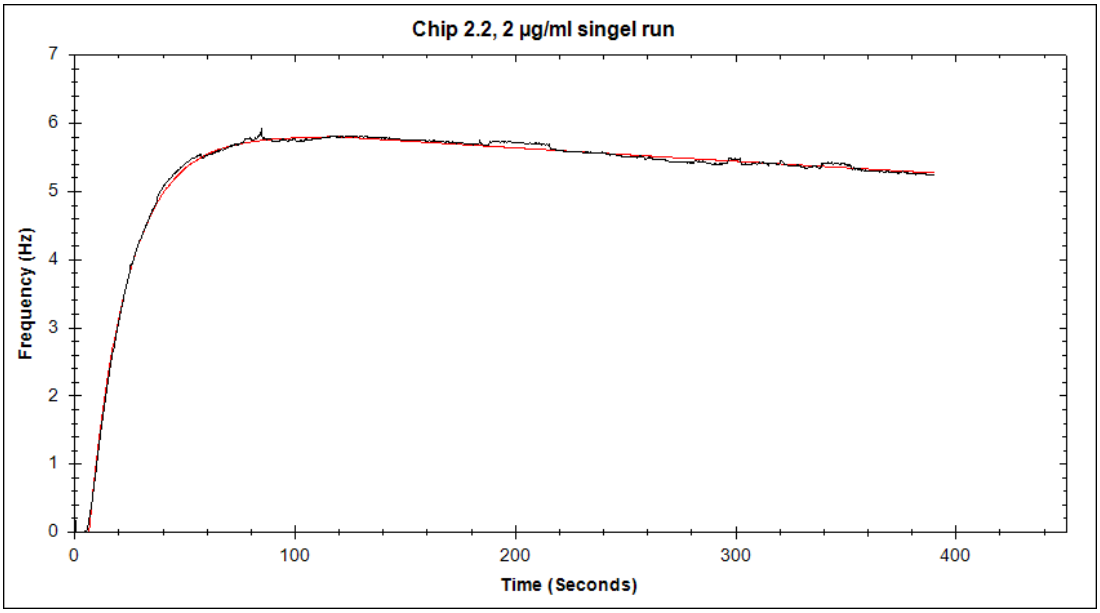

Figure 8. **Sensorgram showing the injection of 2 µg/ml myoglobin over chip 2.2 which has immobilized anti-myoglobin antibody (ab_7005).** The association time is 84s and dissociation time is 300s. The experiment is performed to get estimated kinetic parameters from the interaction. The simulated fitted curve can be seen as the red curve.

Figure 8 show the preliminary run performed on anti-myoglobin myoglobin interaction. The preliminary run was performed on chip 2.2 with 2 µg/ml myoglobin. The curve looks good and the 1:1 fitted simulation fits the raw data well. The kinetic constants extracted was used for simulations and determining the optimal concentrations for the full SCK experiment.

Table 2. **Kinetic data and affinities from preliminary experiment shown in Figure 8.** The binding data is from an 2 µh/ml injection of myoglobin over anti-myoglobin antibody (ab_7005) immobilized surface.

Single run Chip 2.2	
$B_{max}\ (Hz)$	5.84
$k_a\ (M^{-1}s^{-1})$	5.21e+05
$k_d\ (s^{-1})$	4.00e-04

The kinetic parameters from the primary kinetic experiment can be seen in Table 2.

Figure 9**. Simulating sensorgrams using kinetic constants from Table 1 ClampXP**. The six panels show simulated sensorgrams using different concentrations and dilution factors. The concentrations are from top to bottom: 250, 125 and 62.5 nM. To the left the dilution factor is 4 and to the right the dilution factor is 2 for 5 concentrations for each sensorgram. The x-axis is time in seconds and the y-axis is response in hertz.

The output simulated curves with the parameters from Table 2 can be seen in Figure 9. The concentrations used for chip 2.2 and 2.3 is represented by the 125 nM curve with a dilution factor of 2. Chip 2.4 uses the concentrations from simulation with the highest concentrations of 65.2 nM with a dilution factor of 2.

The chosen concentration and dilution factor used for the kinetic experiments for chip 2.3 can be seen in the bottom right position in Figure 9. The 62.5 nM roughly correspond to a highest concentration of 1 µg/ml. The concentration peaks is evenly spread out between a 0 and B_{max}. The simulated curve is close to reach saturation of the surface.

3.1.3 Method verification

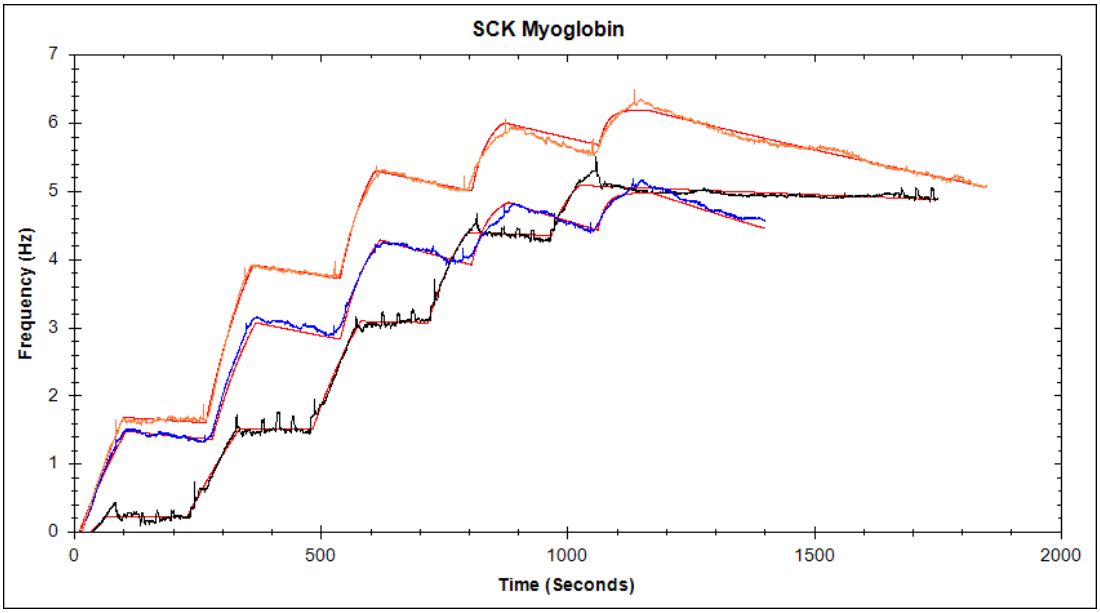

Figure 10**. Three sensorgrams of three SCK experiment with myoglobin and anti-myoglobin (ab_7005) performed on different chips.** Chip 2.2 (orange), chip 2.3 (blue) the concentrations are 2, 1, 0.5, 0.25 and 0.125 µg / ml. For Chip 2.4 (black) the concentrations are 1, 0.5, 0.25, 0.125 and 0.0625 µg/ml. The simulated fitted data can be seen as red curve for each experiment.

Figure 10 show the three SCK runs performed on 3 different chips. Chip 2.3 last dissociation time has roughly been cut in half due to shift in baseline. Note that the fitting is not good in the two highest concentrations. Furthermore, the last dissociation for chip 2.2 fluctuates and does not evenly dissociate, the fluctuation stabilize after 400 seconds. Note that the dissociation for curve from chip 2.4 has not the same dissociation slope as chip 2.2 and 2.3.

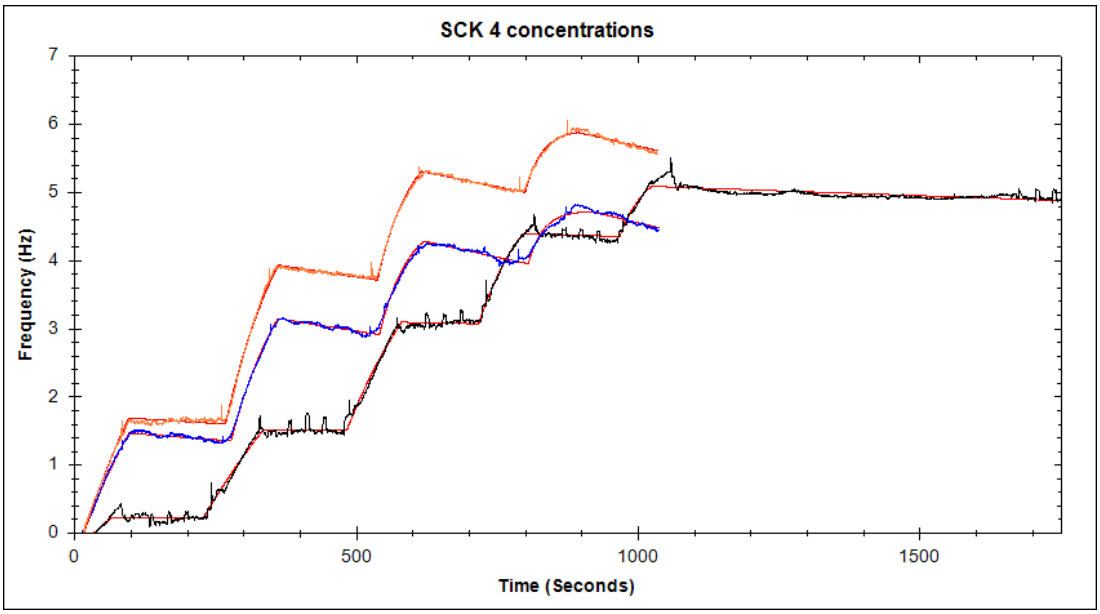

Figure 11 **Three sensorgrams of three SCK experiment with myoglobin and anti-myoglobin (ab_7005) performed on different chips.** The orange curve is from chip 2.2. Chip 2.2 (orange), chip 2.3 (blue) the concentrations are 1, 0.5, 0.25 and 0.125

µg / ml. For Chip 2.4 (black) the concentrations are 1, 0.5, 0.25, 0.125 and 0.0625 µg/ml. The highest concentration from chip 2.2 and 2.3 seen in Figure 10 has been removed. The simulated fitted data can be seen as red curve for each experiment.

Figure 11 show the curves and the simulated fitted curves for the 4 lowest concentrations of chip 2.2 and 2.3. The full SCK data for chip 2.4 is also shown and the highest concentrations for all the curves are the same. Note that the fitting looks much better for chip 2.2 and 2.3 than in Figure 10. The fitting for chip 2.4 is good.

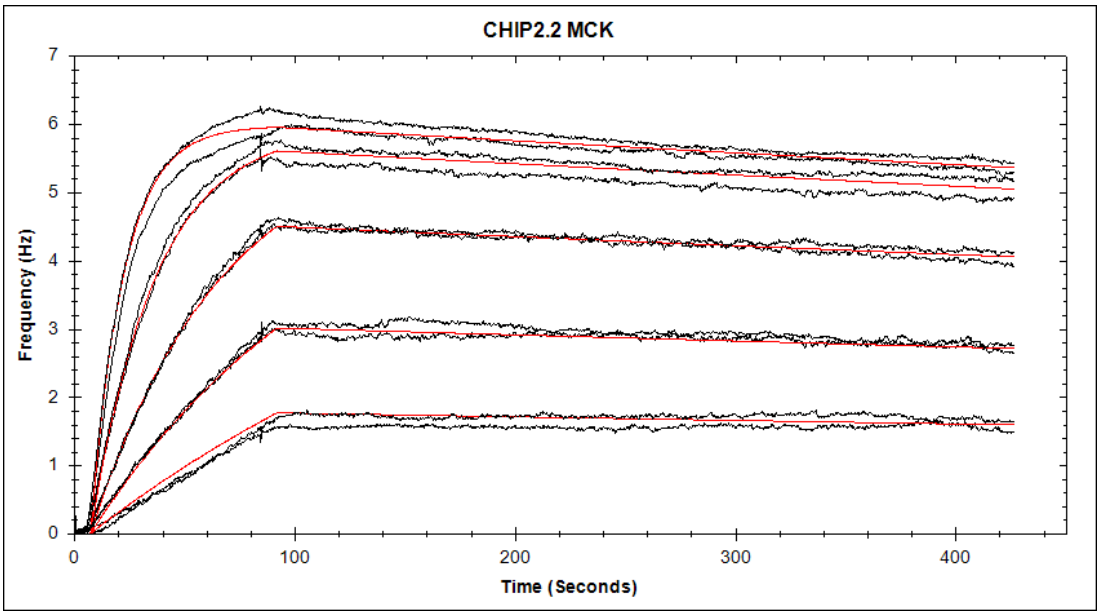

Figure 12. **MCK experiment of myoglobin and anti-myoglobin (ab_7005) from chip 2.2**. The concentrations used are 2, 1, 0.5 0.25 0.125 µg/ml. The simulated fitted data can be seen as red curve for each concentration.

MCK experiment was performed on chip 2.2 as seen in Figure 12. The same concentrations was used as in SCK experiments. As can be seen in Figure 12, the simulated and fitted curve fits well to the data. Note that the fitting deviates the most at the end of the association time for the highest concentration.

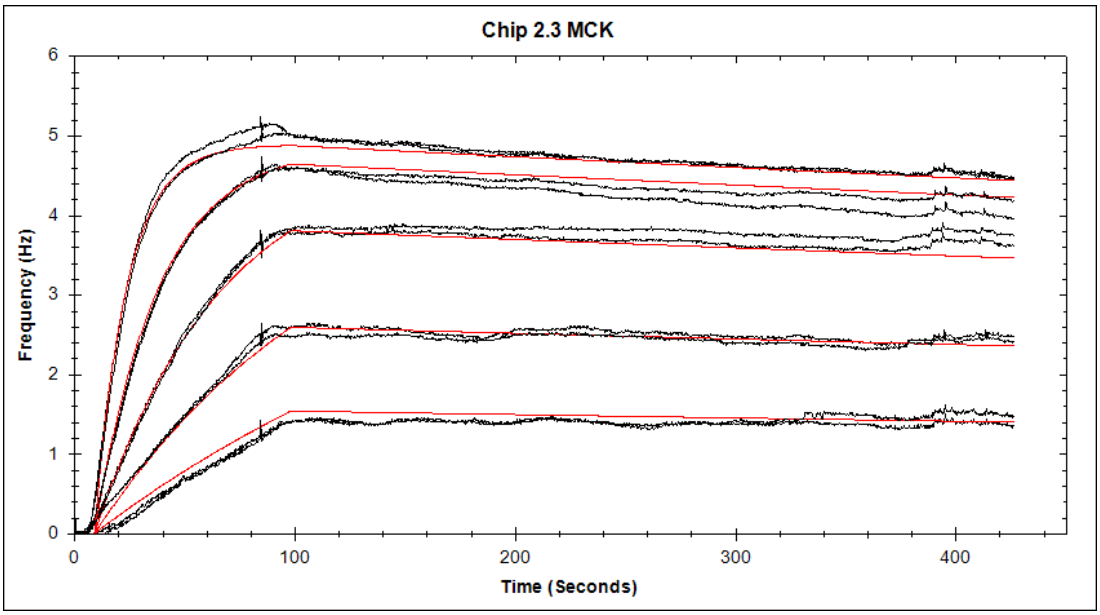

Figure 13. **MCK experiment of myoglobin and anti-myoglobin (ab_7005) from chip 2.3.** The concentrations used are 2, 1, 0.5 0.25 0.125 µg/ml. The simulated fitted data can be seen as red curve for each concentration.

Figure 13 show the multi cycle curves from chip 2.3. The same concentrations was used as in SCK experiments. As can be seen in Figure 13, the simulated and fitted curve fits ok to the data. Note that the worst fitting is at the end of the association phase for the highest concentration.

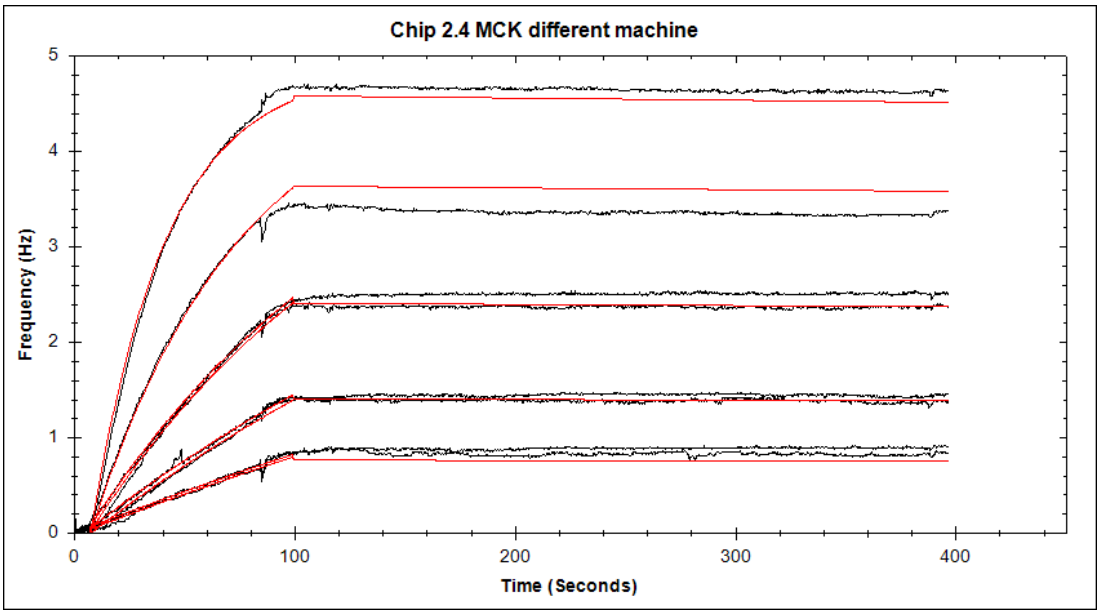

Figure 14. **MCK experiment of myoglobin and anti-myoglobin (ab_7005) from chip 2.4**. The concentrations used are 1, 0.5 0.25 0.125, 0.0625 µg/ml. The simulated fitted data can be seen as red curve for each concentration. Show the multi cycle kinetic run from chip 2.4.

Figure 14 show the multi cycle curves from chip 2.4. The same concentrations was used as in SCK experiments. As can be seen in Figure 14, the simulated fitted curve fits very well to the raw data.

Table 3. **Rate constants and affinities data obtained from Figure 11, Figure 12, Figure 13 and Figure 14 using SCK and MCK methods.**

	Chip 2.2	Chip 2.3	Chip 2.4
		SCK	
B_{max} (Hz)	6.221	5.009	5.397
$k_a\ (M^{-1}\ s^{-1})$	5.36E+05	2.69E+05	3.86E+05
$k_d\ (s^{-1})$	5.85E-05	9.69E-05	1.15E-05
$K_D\ (nM)$	1.093E-10	3.597E-10	2.984E-11
		MCK	
B_{max} (Hz)	5.97	4.78	4.889
$k_a\ (M^{-1}\ s^{-1})$	6.02E+05	6.65E+05	5.42E+05
$k_d\ (s^{-1})$	8.17E-05	1.09E-04	3.32E-05
$K_D\ (nM)$	1.357E-10	1.639E-10	6.126E-11

Table 3 shows the kinetic parameters from the simulated fitted data from all the chips SCK and MCK experiments. The data from chip 2.4 is from a different machine.

3.1.4 Statistical analysis

Table 4. **Statistical analysis on Rate constant data from Table 3.** The table show the average, standard deviation, confident limit and coefficient of variation (CV).

	SCK					**MCK**				
			Confidence limits					Confidence limits		
	Average	StDev	Lower	Upper	CV%	Average	StDev	Lower	Upper	CV%
$k_a\ (M^{-1}\ s^{-1})$	4.0E+05	1.3E+05	2.5E+05	5.5E+05	34	6.0E+05	6.2E+04	5.3E+05	6.7E+05	10
$k_d\ (s^{-1})$	5.6E-05	4.3E-05	7.3E-06	1.0E-04	77	7.5E-05	3.8E-05	3.1E-05	1.2E-04	51
$K_D\ (nM)$	1.663E-10	1.72E-10	-2.9E-11	3.6E-10	104	1.2E-10	5.3E-11	6.0E-11	1.8E-10	44

The average, standard deviation and confidence limit can be seen for both SCK and MCK in Table 4. The CV is a measurement of how much the data deviates within a sample set. The lower the percent the lower the CV is.

Table 5. Show the P-value of T-test between SCK and MCK of k_a, k_d and K_D. The limit is set to P 0.05.

Parameters	P-value
$k_a\ (M^{-1}\ s^{-1})$	0.17
$k_d\ (s^{-1})$	0.03
$K_D\ (nM)$	0.60

Student T- test was performed in excel between the parameters from the SCK and MCK experiments. As can be seen in Table 5, the null hypothesis is true for k_a and K_D. The confident

limit was set to 0.05. The k_a and K_D has a P-value over 0.05 indicating that the results from the SCK and MCK methods are similar.

Table 6. **The output from the two-factor ANOVA with replication analysis of the kinetic constants in Table 3 performed in EXCEL.** The P-value was set to 0.05.

ANOVA

Source of Variation	*SS*	*df*	*MS*	*F*	*P-value*	*F crit*
Sample	2.12E+10	1	2.12E+10	5.90	0.032	4.75
Columns	9.99E+11	2	4.99E+11	138.8	5.1E-09	3.89
Interaction	4.25E+10	2	2.12E+10	5.90	0.0164	3.89
Within	4.32E+10	12	3.60e+10			
Total	1.11E+12	17				

An ANOVA analysis was performed on the data set. The sample row describes the difference between methods and the columns row describes the difference between the chips. SS is Sum of Squares, df is degrees of freedom, MS is Mean Square and F is F-statistic. The result show that the methods are not significant similar because the P-value is lower than 0.05 in the sample row (Table 6).

3.1.5 Time difference between SCK and MCK

Table 7. **The experiment time from the initial injection to the end of regeneration time**. The experiments can be seen by looking at programmed C-fast list can be seen in Appendix 3.

Method	Experiment time
MCK	8714 s
SCK	2691 s

Table 7 show the time the experiment time for MCK and SCK experiments. The time is taken from the first injection to the end of the regeneration wait time. As seen in Appendix 3, each regeneration has a waiting time of 600s to stabilize the baseline. When regeneration is impossible or unnecessary, the time will be 1850s without regeneration. The SCK experiment is 3.24 times faster than MCK experiment.

3.2 Nanoparticles

3.2.1 100 nm polystyrene nanoparticle

3.2.1.1 Immobilization

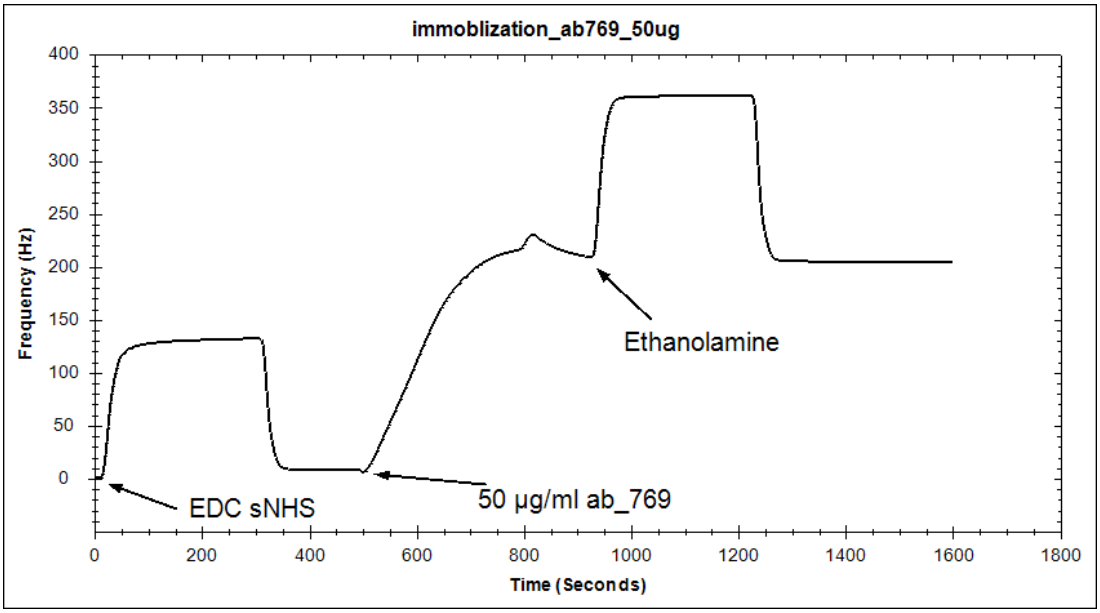

Figure 15. **Sensorgram of the immobilization of anti-transferrin (ab_769) with amine coupling.** First an injection of EDC and sNHS was injected for 300s. Then 50 µg/ml anti-myoglobin was injected for 300 s. The surface was then deactivated by injecting ethanolamine for 300s.

The immobilization of anti-transferrin (ab_769) can be seen in Figure 15. The resulting immobilization equals to 200 Hz. The immobilization curve looks normal.

3.2.1.2 SCK sandwich assay experiment

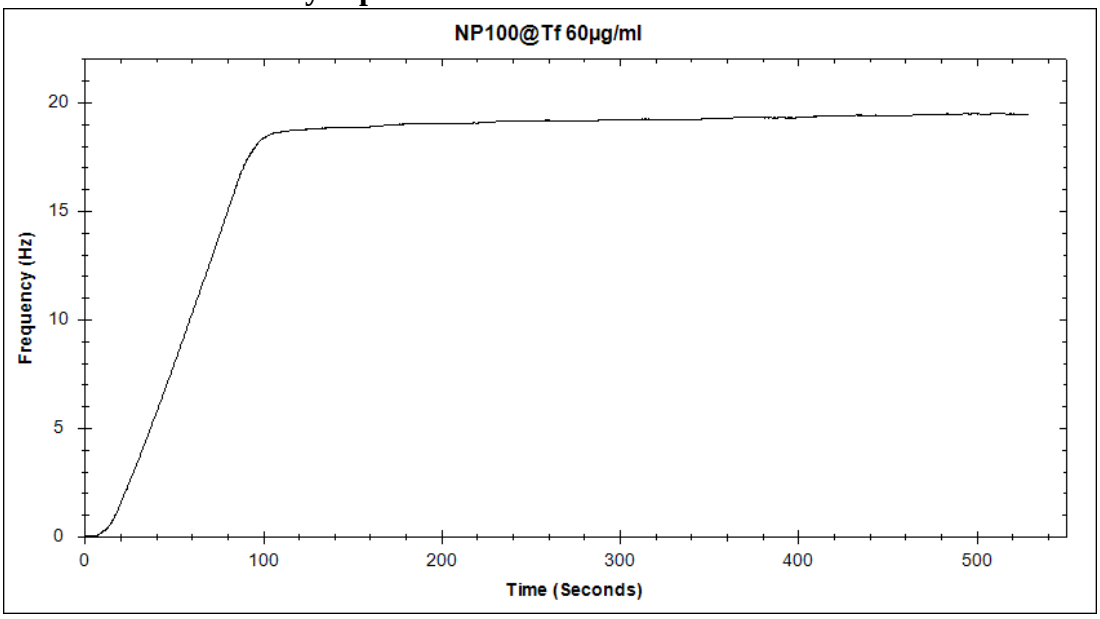

Figure 16**. Sensorgram of the attachment of NP100@Tf by single injection of 60 µg/ml 100 nm transferrin coated polystyrene nanoparticle on chip.** The association time is 84 s.

The binding of NP100@Tf to chip surface can be seen in Figure 16. The total response is estimated to 19 Hz. Note that dissociation phase has a positive derivate.

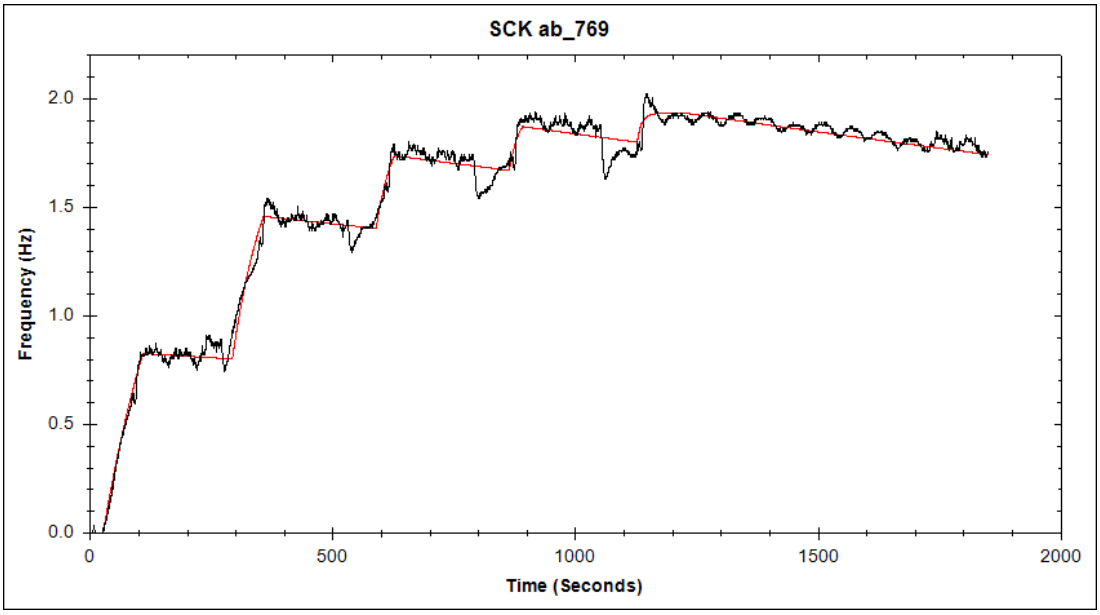

Figure 17. **Sensorgram of the SCK sandwich assay experiment performed on attached NP100@Tf.** The analyte is transferrin and the concentrations are 30, 10, 5, 2.5 and 1.25 µg/ml. The simulated fitted data seen be seen as red curve.

The resulting SCK sandwich assay experiment can be seen in Figure 17. The noise level is very high during the association phase and the curve fluctuates during the whole experiment. One can see that the surface reaches close to saturation in the last two injections of analyte.

Table 8. **The kinetic constants extracted from the SCK sandwich assay experiment seen in Figure 17.**

NP100@Tf Sandwich assay	
B_{max} (Hz)	1.94
k_a $(M^{-1}s^{-1})$	8.21e+05
k_d (s^{-1})	3.264e-05

The kinetic parameters from the NP100@Tf sandwich assay can be seen In Table 8. The important data is the B_{max} parameter.

3.2.1.3 100 nm polystyrene nanoparticle calculations.

The calculations can be seen in appendix 1

The resulting anti-transferrin antibody (ab_769) per 100 nm polystyrene nanoparticle is:

$$\frac{N_{ab\_769}}{N_{NP100@Tf}} = \frac{5.44 * 10^9}{1.94 * 10^8} = 28\ ab_{769} per\ NP100@Tf$$

This is roughly half the value of the reference value.

3.3 Cell counting

3.3.1 Image analyze of images from 2 chips.

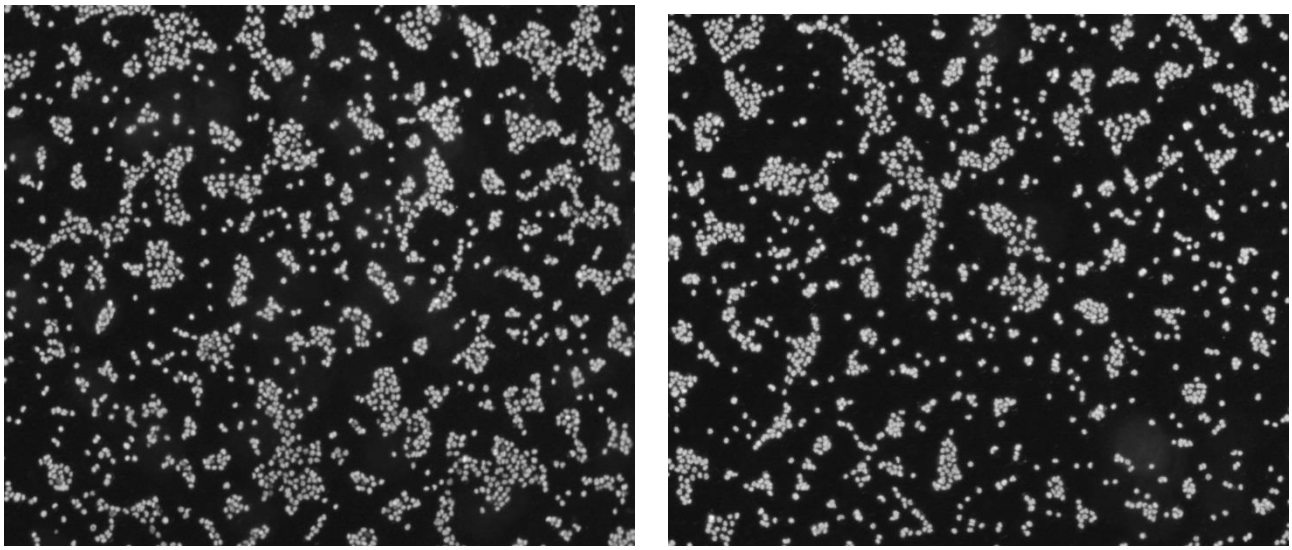

Figure 18. **Images shows image of two different chips with stained cells immobilized.** The images is taken with Nikon eclips 80i microscope on 4X magnification. The image of Chip 1 is to the left and Chip 2 is to the right.

Analysis of two images containing immobilized (Figure 18). Note that Chip 2 image in Figure 18 has less cell density than Chip 1.

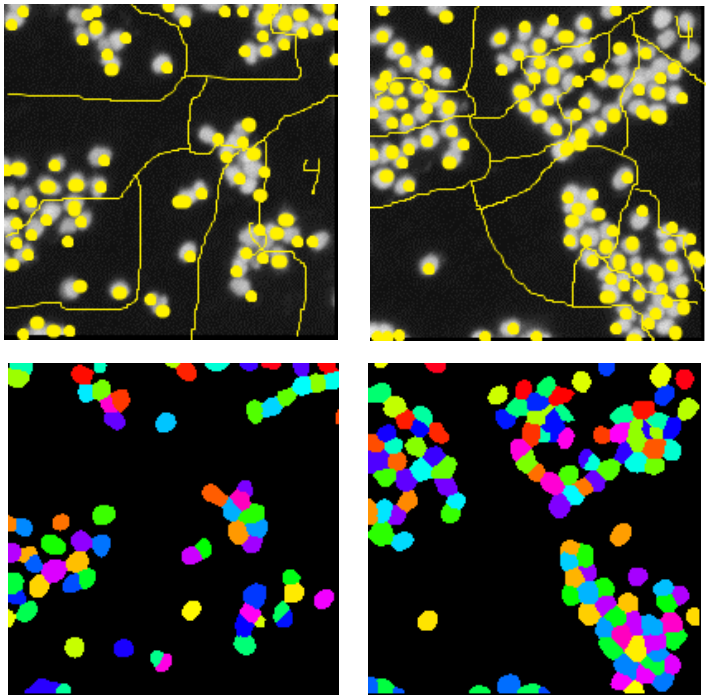

Figure 19.**Manually and automatically counted images from cropped 200x200 pixels from images in Figure 18**. Chip 1 is to the left and chip 2 is to the right seen in Figure 18. The cropping was done in the upper left corner of both images. Both images where manually counted and 74 cells where counted in the upper left image. Both lower images show the objects identified when D_{min} was set to 4.

The images from figure 6 was cropped 200x200 pixels in the upper left corner of the images. The cropped images were manually counted. Every dot represent one cell and every encirclement represent 10 cells as seen in Figure 19. Chip 2 has the highest density in the cropped image seen in Figure 19 but lowest density in the original image seen in Figure 18. The Automatically and manually identified nuclei match well when comparing the upper images with the lower in Figure 19. The error of the automatically cell count is 1.3% for chip 1 and 3.5% for chip 2 in comparison with the manually counted.

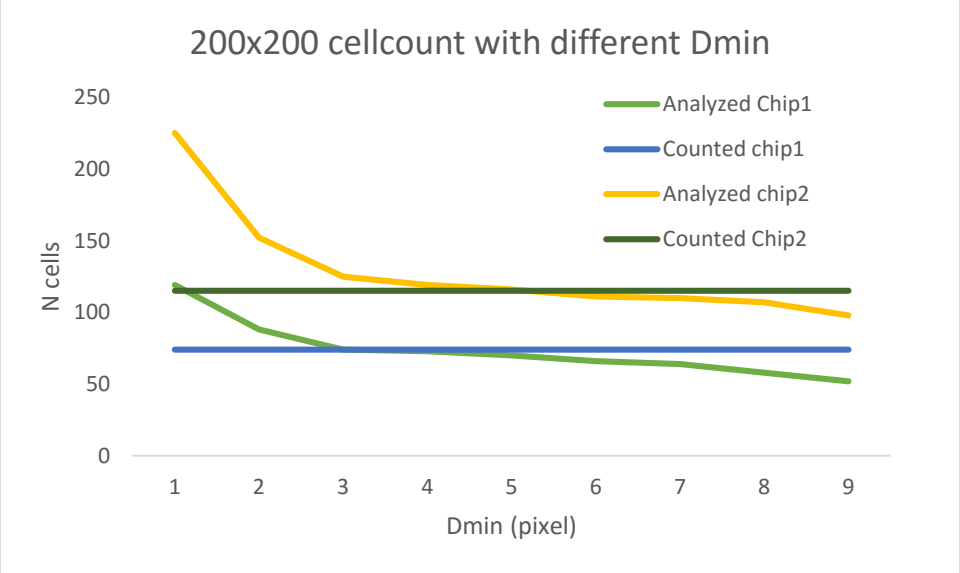

Figure 20. **The counted number in the cropped 200x200 images seen in Figure 19 (green, blue).** The yellow curve show the number of cells counted with different D_{min} of the of the 200x200 pixel cropped image of chip 2. The light green curve show the number of cells counted with different D_{min} of the 200x200 pixel cropped image of chip 1. Both was analyzed using "DminAnalyzer" pipeline.

Figure 20 show the images in Figure 19 analyzed with the "DminAnalyzer" pipeline. Chip 1 has the same cell count when D_{min} is set to 5. Chip 2 has the same cell count when D_{min} is set to 3. Note that D_{min} is not the same for both of the chips.

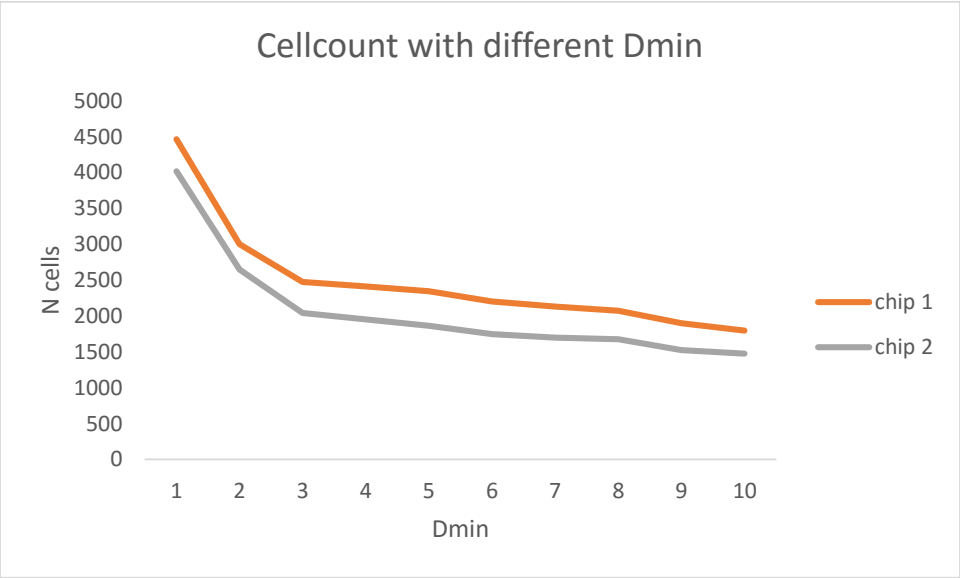

Figure 21. **Result from "DminAnalyzer" pipeline on the whole chip.** The cell count was done with different D_{min} ranging from 1 to 9 on both images.

Both whole images was analyzed with "DminAnalyzer" pipeline as seen in Figure 21. Note that the shape of the curves in Figure 21 is very similar to the shape of the curve in Figure 20.

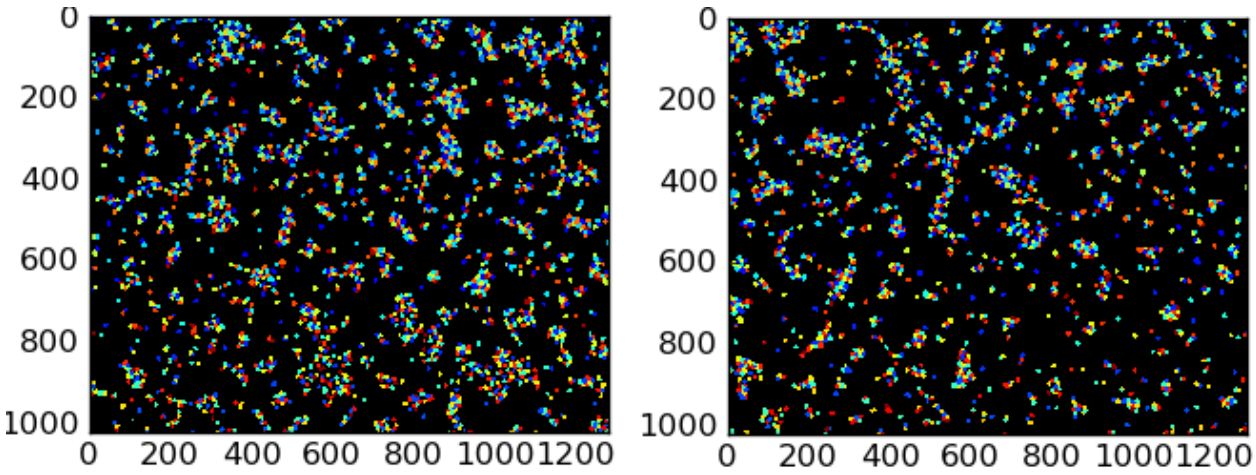

Figure 22. **The objects identified rith the CellCount pipeline from images in Figure 18 with a a D_{min} of 4 pixels**. Each dot represents one identified cell.

Figure 22 show an output image showing the identified cell nuclei. Figure 22 is very similar to the original images seen in Figure 18.

Table 9. **The output parameters from the "CellCount" pipeline.** The accepted object parameters show how many cells where identified.

Parameters from Cellprofiler	CHIP1	CHIP2
Threshold,	0.357	0.38
# of accepted objects	2413	1952
10th pctile diameter (pixels)	9.1	9.1
Median diameter (pixels)	11.6	11.6
90th pctile diameter (pixels)	13.8	13.7
Area covered by objects (%)	19.8	16
Thresholding filter size	1	1
Declumping smoothing filter size	2.7	2.7
Maxima suppression size	2.7	2.7

The result of the cell count on both images can be seen in Table 9. Chip 1 has higher density than chip2. Table 9 also contains several other output parameters that CellProfiler provides.

3.3.2 Nikon eclips 80i microscope image size an relation to chip surface

Table 10. **The image size of the Nikon eclips 80i microscope and the relation to the Attana's chip sensor surface.** The image size for each magnification was calculated and related to the sensor area of the chip. Number of images needed to be taken to get accurate cell count was calculated with (Equation 1) with 0.01 accuracy.

Zoom	pixel scale (µm/pixel)	x (pixel)	y (pixel)	N (pixel area)	Area per image (m)	Area of chip (m)	Achip/Aimage	N_image0.01
2x	3.19	1280	1024	1310720	1.34E-05	1.59E-05	1.19	0.0015
4x	1.6	1280	1024	1310720	3.36E-06	1.59E-05	4.74	0.0059
40x	0.16	1280	1024	1310720	3.36E-08	1.59E-05	473.86	0.59
60x	0.11	1280	1024	1310720	1.59E-08	1.59E-05	1002.53	1.25

Table 10 show the area of images with different magnification of the Nikon eclips 80i microscope and how many times you need to multiply the area of a image to get the area of the whole chip. The result from equation 1 using e = 0.01 can be seen in the last column. Note that it requires less than one image for 2x, 4x and 40x magnification to get accurate cell count.

3.3.3 Method verification for proposed image analysis process

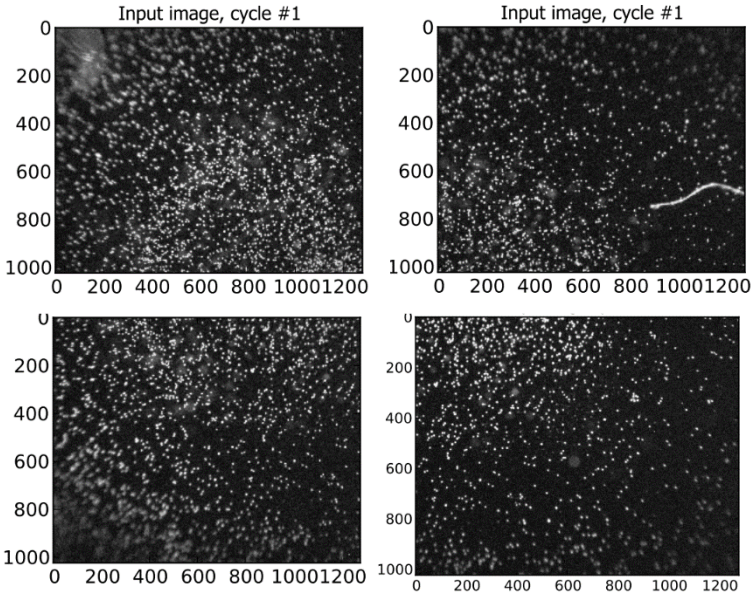

Figure 23. **Four images taken with Nikon eclips 80i microscope on 4X magnification on Attana's chip with suspended stained cells according to method described in Figure 5.** The scale on the side show the number of pixels.

The images in Figure 23 is taken according to the method described in Figure 5. Note that the two left images have a higher cell density than the two right images. The two lower images has an overlap of around 500 px. The two top images is harder to see but have roughly the same overlap. This is in line with the prediction seen in Figure 5.

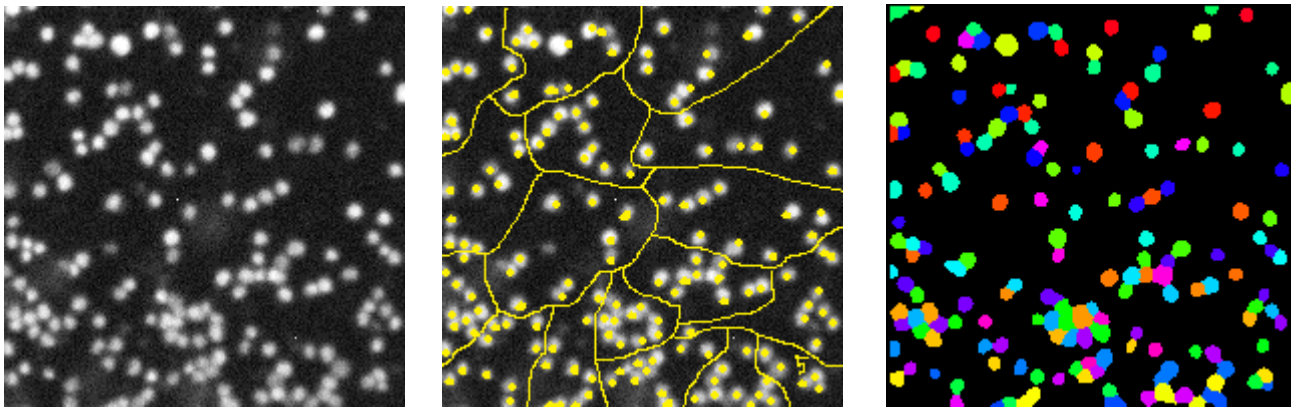

Figure 24. **The cropped 200x200 image (left) is from the lower right corner of the upper left image seen in Figure 23.** The same manually counted image in the middle. 165 cells where counted. The right image show the objects detected with the D_{min} set to 3. The 200x 200 cropping was done in the lower right corner of the image for optimal contrast

The top left image from Figure 23 D_{min} was determined with "DminAnalyzer" pipeline. The resulting cropped image can be seen in Figure 24. The cells is easily distinguishable and was counted manually. The resulting cell count is 165 cells. The nuclei identified with D_{min} set to 3 can be seen in the right image in Figure 24. The automatically cell number when D_{min} set to 3 is 161. The error of the automatically cell counted is 3.1% in comparison with the manually counted. Note that the manually counted and automatically counted nuclei match almost exactly.

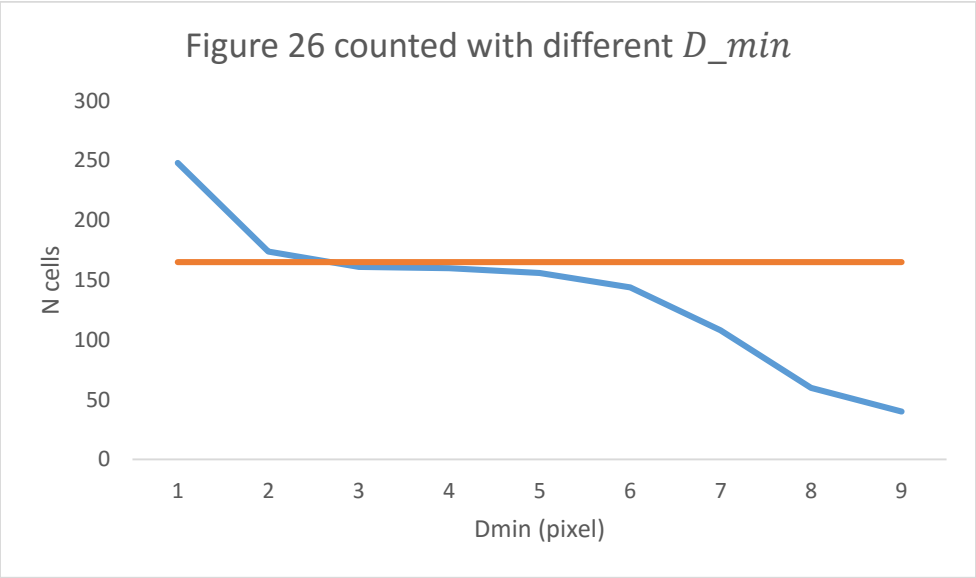

Figure 25. **The cell count with a D_{min} ranging from 1 to 9 (blue).** The red curve represents the manually counted cell number seen in figure 13.

The resulting cell count for each D_{min} can be seen in Figure 25. The closest D_{min} cell count to the manually counted number is when D_{min} is equal to 3.

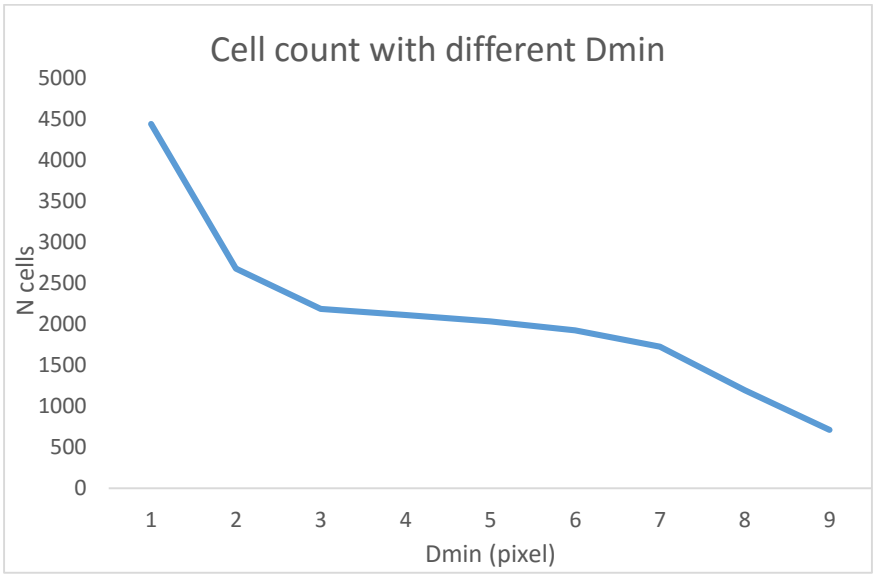

Figure 26. **The cell count for a D_{min} ranging from 1 to 9 pixels for the whole image in the upper right image in Figure 23.**

The whole image was analyzed with the "DminAnalyzer" pipeline. The resulting curve can be seen in Figure 26. Note the similarity between Figure 25, which is analyzed a part of the image, and Figure 26 that is analyzed the whole image.

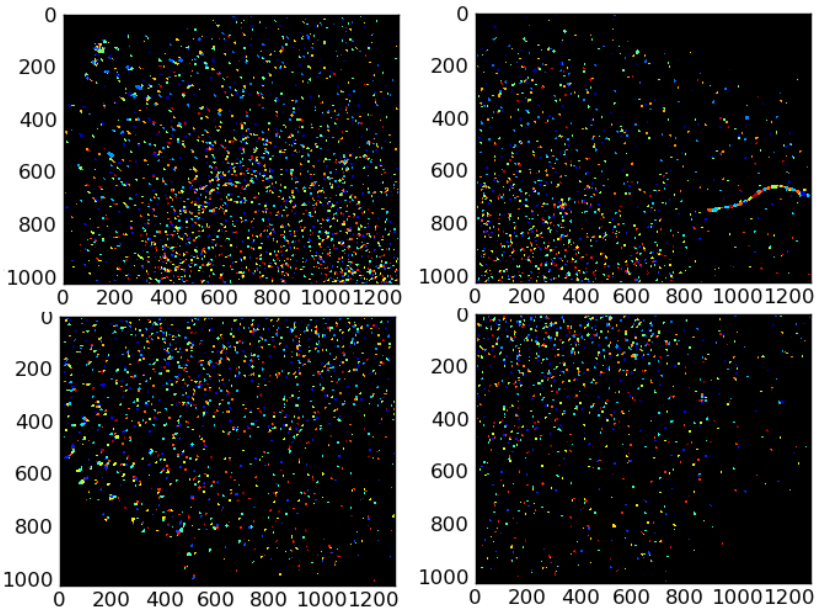

Figure 27. **The objects identified rith the CellCount pipeline from images in Figure 23 with a a D_{min} of 3 pixels.** Each dot represents one identified cell.

Nuclei's detected and their locations can be seen in Figure 27. The nuclei distribution is roughly the same as the original image. No nuclei was identify where the image was out of focus which can be seen in the outer corner of the images seen in Figure 27.

Table 11. **The cell count from each image from Figure 23.** The cell count is a result from the "CellCount" pipeline and the output is cells that touch borders and not touch borders. The average is calculated and the number of cell on whole chip is calculated by multiply the mean value with 4.

image	N cells not touching border	N cells including touching border
Upper left	2160	2189
Upper right	1173	1203
Lower left	1408	1444
Lower right	979	1006
Mean value	1445	
N cells on whole chip	6849	

Table 11 show the result from the "CellCount" pipeline when analyzing the images from Figure 23. The data was extracted and average calculated using the "CellCountCompiler" script. Number of cells for the whole chip was calculated by multiplying the mean value from all the images with the Achip/Aimage value in Table 11. The resulting cell number represent all cells on the whole of the chip.

4 Discussion

4.1 SCK

The purpose of this section of the report is to establish and validate a method to perform SCK experiments Attana's QCM biosensors so it can be applied on nanoparticles. SCK methodology can radically improve Attana's biochemical and cell based assay. A higher throughput will be possible by the lower experimental time and the streamlined experimental design. Furthermore, it will be possible to perform interaction analysis on interaction not possible before due to problem with regeneration. Therefore it is optimal to use on the Nanoclassifier project to characterize nanoparticles.

4.1.1 Immobilization

The immobilization of anti-myoglobin can be seen in Figure 7. The procedure has a normal variation that can be seen in the difference immobilization. The surface density of around 30 Hz used in this experiment is lower than previously tested to counteract mass transport limitation. The lowering of the surface density resulted in the mass transport constant was eliminated.

The immobilization follows the SCK obtained data seen in Table 3. Chip 2.2 has the highest B_{max} then chip 2.4 and chip 2.3 respectively. The same pattern can be seen in immobilization Figure 7. This shows that the immobilization and kinetic experiments behaves as expected in regards of B_{max}. The difference in response influences B_{max} but the overall kinetic interaction is the same.

4.1.2 SCK experiment methodology

The preliminary experiment can be seen in Figure 8 and the resulting kinetic constants from the initial single injection are shown in Table 2 and were calculated using ClampXP and a 1:1 interaction model. Comparing the preliminary data seen in Table 2 with the resulting data seen in Table 3, the association rate are similar but the dissociation rate are higher in the initial data set than in the final data even if the data diverge, the initial parameters are still a good indication of how the final experiment will look like and functions as a rough estimate sufficient to use for experimental planning.

The second step is to simulate curves with different concentrations and dilution factor using the parameters from the single run. The curves can be simulated with any concentration or dilution factor. In this case the simulations was performed on concentrations of 250, 125 and 62.5 nM with dilution factor of 4 and 2 with a 1:1 binding model. The simulations can only be done in sets of 6 due to limitations of ClampXP. The dilution factors and concentrations simulations where chosen to be as general as possible and cover a broad range of interactions. The concentration should be as low as possible due to the cost and possible scarcity of the analyte. The simulations can be performed with 1:1, mass-transport limitation and 2:1 binding models. This gives the opportunity to simulate and plan a broad range of interaction experiments.

The chosen concentrations for chip 2.2 and 2.3 experiment was set to 112.4 nM with a dilution factor of 2 as seen in Figure 10. This is a concentration of 2 µg/ml myoglobin and is roughly equivalent to the 125 nM simulation seen in Figure 9. The reasoning for choosing 2 µg/ml was that the curve reaches saturation of the surface and the response for all concentrations is evenly distributed between 0 and B_{max}. This was later changed to 1 µg/ml for chip 2.4 to solve the problem with oversaturation of the surface.

The whole SCK experiment from all three chips can be seen in Figure 10. The simulated fitted curve doesn't fit the data well and a preliminary analysis show the kinetic parameters from the whole experiment is not significant similar to the equivalent MCK kinetic parameters. The solution was to remove the highest concentration and the result can be seen in Figure 11. The simulated fitted data fits the experimental data much better in Figure 11 than in Figure 10. The resulting parameters from Figure 11 is much more similar to the MCK kinetic parameters are shown in Table 3.

4.1.3 MCK experiments

The MCK data from each chip has be seen in performed on the same machine in Figure 12 and Figure 13. The last MCK experiment seen in Figure 14 was performed on a different machine. This was because complication with the machine and time constraints. The resulting data is therefore comparable but with the additional error of producing the data on a different machine. The simulated fitted data fits the curves well. The variation seen in the dissociation phase can be as a result on deviation on the reference surface or due to the low surface density. The simulated fitted data is the worst at the end of the highest concentration of the association phase. The reason is oversaturation of the surface due to too high analyte concentration. This is compensated by the lower concentration and the resulting kinetic constants are more accurate. The resulting kinetic parameters can are shown in Table 3.

4.1.4 The difference between SCK and MCK experimental error

The difference between 4 or 5 concentration SCK experiment from chip 2.2 and 2.3 show that SCK experiments is much more sensitive than MCK experiments. Because it's a continuous experiment, any shift of the baseline will ruin the whole experiment and not only one concentration cycle. The problem in this case is that the injection of the highest concentration result in an oversaturation of the surface. All binding sites are already occupied by analyte in the SCK experiment and by injecting a high concentration oversaturation of the surface occurs. This is the case when the response to concentration ratio is very low. The solution is to not inject a high concentration when the response level is already close to B_{max}.

Another problem with SCK is that the same concentration error impacts SCK experiment more than MCK experiments. By comparing the orange SCK curve in Figure 10 and the equivalent MCK experiment in Figure 12, one can see that they have the same error. The end of the association time in MCK experiment doesn't fit with the simulated fitted data indicating that the last concentration is too high. The association up to that point fits the data well. The last concentration in the SCK experiment is added to an already partially saturated surface that has a frequency of 5.5 Hz. The simulated fitted curve in Figure 12 deviates from the experimental data

starting around 5.5 Hz for the highest concentration. This means that the highest concentrations in the SCK experiment results in an error impacting the kinetic constants of the interaction. Furthermore, the highest concentration results in fluctuation of the dissociation which result in error in the dissociation rate constant.

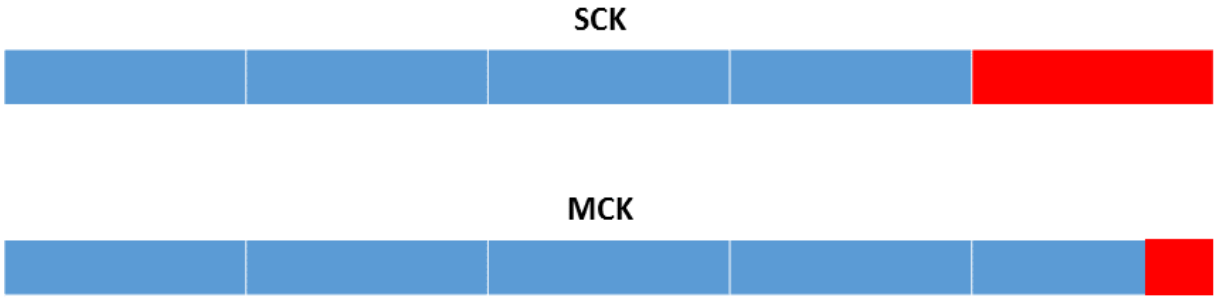

Figure 28. **Schematic visualization of the error on difference of the SCK and MCK with to high concentration.** Each "block" represents association time for the 5 concentrations. The red indicate the error in the association time.

The reason why the SCK parameters deviates from the MCK parameters is because higher error in SCK experiment when using high concentrations. If the resulting data of one concentration is inaccurate, its 1/5 of the association rate data. In contrast, the MCK start from an unoccupied surface which results in correct association until surface is oversaturated. This results in association constant which is approximately 1/15 inaccurate. The difference is visualized in Figure 28. The reason SCK parameters is inaccurate with high concentrations is because the resulting error is higher in SCK due to an already occupied surface.

The resulting parameters from SCK and MCK experiment from all three chips can be seen in Table 3. The constants is relative similar to each other. The k_a has a higher cause of deviation because the k_a parameter reaches the limit of detection for the Attana A200 machine. This could cause a higher error in the k_a parameter. The k_d should be more accurate due to the long last dissociation time and that dissociation rate is concentration independent. But when comparing chip 2.2 and 2.3 with chip 2.4 can see that the data from chip 2.4 result in a lower dissociation. This is a result of producing the data on a different machine and problem with baseline together with interference. If the baseline on the reference chip and the experiment chip doesn't match it will result in inaccurate dissociation constant. Furthermore, the dissociation rate is very low for and a small difference in baseline can impact the dissociation constant greatly. The B_{max} is relative low and therefore experimental noise will impact the result more. The low dissociation rate can also make it difficult to distinguish between dissociation and drift. This could also be a cause for deviation of dissociation constant.

4.1.5 Time saves

One important advantage for SCK experiment is the amount of time saved. As seen in Table 7, SCK is 3.24 times faster than MCK. SCK is therefore more suited for high throughput due to its shorter experiment time. With shorter experiment time several different analyte can be tested in succession fast. With fewer regeneration each chip can perform more experiments. Furthermore, Attana's cell based assay would greatly benefit using SCK methodology due to very long

experiment time. The cell based assay can take days to complete with MCK due to long time for baseline to stabilize after regeneration. With SCK the time to perform a cell based assay would be greatly reduced.

4.1.6 Statistical analysis

A two-factor ANOVA with replicates analysis was performed on the kinetic constants seen in Table 3. The analysis was performed in Excel and the results can be seen in Table 6. The analysis is a two-factor analysis with replication and the P-value should be greater than 0.05. This analysis measure if the variance is between and within the methods. This show if the methods is produce significant similar kinetic constants. The methods don't produce significant similar result as seen in Table 6. The sample rows column has a P-value lower than 0.05 which indicate that the null hypothesis can be discarded. This show that the methods are not significantly similar.

To evaluate which kinetic constant deviates in the different methods a Student t-test was performed on the dataset in Table 3. The result from the analysis can be seen in Table 5. The P-value should be greater than 0.05. The test show if the kinetic parameters produced by the different methods are significant similar to each other. The result show that the k_a and K_D is significant similar to each other. The k_d has a P-value lower than 0.05 and therefore can the null hypothesis be discarded. Therefore it is the k_d constant that results in the failure of the ANOVA analysis. The k_d deviates because data from Chip 2.4 is from a different machine and that the baseline of the reference and experiment channel doesn't match. This could be solved by using the same machine and make sure that the baseline match between the channels.

4.2 Nanoparticles

4.2.1 100 nm polystyrene nanoparticles

4.2.1.1 Immobilization

The immobilization of anti-transferrin can be seen in Figure 15. The immobilization was performed with 50 µg/ml of antibody. This is a very high concentration and the resulting surface density is high. The high surface density has been used for previous MCK sandwich assay experiment. This immobilization resulted in a four times higher surface density. Even if the surface density is higher than previous experiment it should function due to the ability to control the density of secondary ligand by changing nanoparticle concentration.

4.2.1.2 Nanoparticle attachment

The attachment of nanoparticle to the surface can be seen in Figure 16. Figure 16 show the injection of 60 µg/ml 100nM transferrin coated particle. The resulting response is roughly 19 Hz. It's important to attach sufficient amount of particle so the SCK experiment result in high enough response. If immobilization is to low, then the SCK will have lower response and might be more sensitive to noise. If the surface density is too high the analyte will not be able to attach on all epitopes due too little to no room between nanoparticles. Therefore it's very important to find the optimal surface density of secondary ligand.

4.2.1.3 SCK experiment

The SCK experiment performed after attachment of NP100@Tf can be seen in Figure 17. The analyte buffer and running buffer has different composition resulting in a peak at the end of the association time. This would normally been removed by subtracting the reference channel, but the reference channel and experimental channel doesn't match resulting in bad curve.

The saturation of the surface can still be extracted from the graph with relative accuracy. By looking at the Figure 17, the higher concentrations response level indicates saturation of the surface, due to lower response after increasing concentration injection. Because the purpose of the experiment is the measure the number of epitopes, saturation of the surface means that all epitopes are bound with antibodies. By knowing the weight of a nanoparticle and the weight of an antibody calculation of antibodies per nanoparticle can be calculated. Furthermore, the antibodies is attached to an epitope, therefore is antibodies per nanoparticle the same as epitope per nanoparticle.

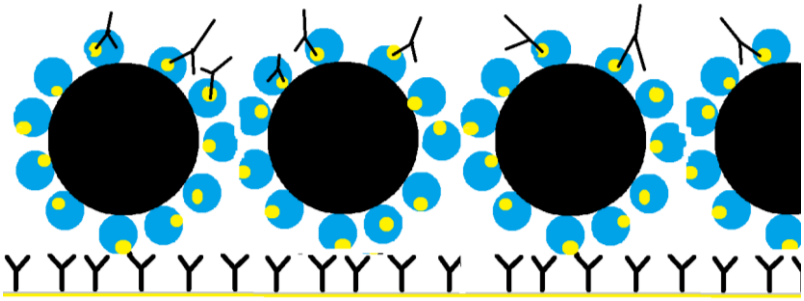

Figure 29. **Schematic representation of a dense nanoparticle surface.** The nanoparticles are too close together and will not allow analyte to get to all binding places. This results in lower response of analyte.

The calculated epitopes per nanoparticle is 28 as seen in section 3.2.1.3 and calculation can be seen in Appendix 2. The reference number for available epitopes per NP100@Tf is 62 calculated in Appendix 2. The result is roughly half and therefore not accurate. This can be a result of too high NP100@Tf density of the surface which result that the analyte will not attach to all available epitopes as seen in Figure 29. Lowering ligand density or nanoparticle density on the surface would be a possible solution. Another possible solution would be to lower the flow rate which enables the analyte to diffuse more, reach deeper and attach to all available epitopes. Avidity could be the reason for the error. If all of the antibodies binds to two epitopes the resulting response will be half.

The preparation of nanoparticles can be a source of error. Because there are no centrifuges with sufficient rcf in the lab in Stockholm, I was forced to prepare the nanoparticles in Uppsala. The transportation back and forth could influence the nanoparticles. For example, if the excess transferrin is not removed they can attach to the surface and hinder the attachment of nanoparticle. Furthermore, the attached protein would be included in the attached mass and therefore skew the antibody nanoparticle ratio. Therefore it's important to prepare the nanoparticles accurately.

By comparing nanoparticle SCK experiment seen in Figure 17 with myoglobin experiments in Figure 10 one can see that both have the same shape. This proves that SCK sandwich assay

experiments can be used on nanoparticles. Further experimental optimization is needed to achieve the same results as in the reference data.

4.2.2 High throughput nanoparticle characterization

This method has high potential to enable high throughput nanoparticle characterization. By no need of surface regeneration, a wide range of interactions can be tested. I have proposed a modified experimental design seen in Appendix 4. This SCK experiment first attaches the nanoparticle, then lower the flowrate and perform the SCK experiment. The dissociation times is extended due to the lower flowrate. This experimental design seen in Appendix 4 was meant for characterize NP200@Tf but due to lack of time was not able to test. This experimental design can be applied to a variety of nanoparticles and could be used as a standard experiment for nanoparticles.

4.3 Cell counting

4.3.1 Images from 2 separate chips

Analyzation was performed using images (Figure 18) of immobilized cells on Attana's COP-a sensor chip. The cells are very well defined and the background is relative homogenous. Manually counting the cells on the whole images would take too much time. Instead the images was cropped to 200x200 pixel size and the resulting image can be seen in Figure 19. This is done automatically by the "DminAnalyzer" pipeline. This was done to save time and more easily count the cells as a reference to determine the D_{min} of the nuclei.

The cropping is a part of the "DminAnalyzer" pipeline and the result can be seen in Figure 20. It's interesting to see that chip 1 has a D_{min} of 3 and the chip 2 has a D_{min} of 5. The cells are from the same cell line and immobilized for the same experiment and therefore should have the same D_{min}. This is most likely a result of a manually counting error or possibly the cells are more clumped on Chip 2. When comparing the automatically identified nuclei with the manually counted seem to be very similar, as seen in Figure 18. To compromised, the D_{min} was set to 4 in the "CellCount" pipeline. The resulting error is 1.3% for chip 1 and 3.5% for chip 2. This also very low and if the D_{min} was set individually the error would lower.

When comparing the cropped "DminAnalyzer" data with the whole image there are similarities. The "DminAnalyzer" data for the whole image can be seen in Figure 21. When comparing to Figure 20 you see that the curves has the same basic shape. This indicates that the cropped "DminAnalyzer" data represents the whole image or chip well.

The result of the "CellCount" pipeline can be seen in Figure 22 and Table 9. When looking at Figure 22, which show the identified cell nuclei, the distribution is the same as in the original image seen in Figure 18. This is further shown in Figure 22 which show the identified cell nuclei on top of the original image. This indicates that the cell count is accurate.

The resulting cell count can be seen in Table 9. The cell density on chip 1 is higher than chip 2 which is in line by looking at the images in Figure 18. In addition to cell count, CellProfiler calculates additional parameters. The median diameter can probably be used to predict D_{min} with

a certain accuracy without using “DminAnalyzer”. Area covered by objects can be used to determine confluence on the chip if the cell membrane is stained in addition to the cell nuclei. The number seem accurate enough to do another experiment which analyses several images from the same chip.

4.3.2 Microscope parameters

To determine the cell number for the whole chip you multiply the area of the image so it represents the area of the chip. This can be done by knowing the area of the images and the area of the chip. Nikon eclips 80i microscope with 4x magnification was used and he resulting image area was calculated and can be seen in Table 10.

The number of images required to get an accurate cell number was calculated with (Equation 1) and can be seen in Table 10. The 4x magnification resulted in image number necessary for an accurate cell count well below one. The article describing the method has a bigger surface and smaller image area. This results in a bigger chip to image area ratio. In comparison the chip to image ratio for 4 x magnification with Attana’s chip which is 4.73, seen in Table 10. The chip image ratio is very low in comparison with the article that has a chip to image ration in the hundreds. Furthermore, the article study *Escherichia coli* which is significant smaller than mammalian cells used in this report [16]. The seeding used in the immobilization protocol uses a low concentration of cells. All this combined results that only one image is required to get an accurate cell count.

4.3.3 Method verification experiment

As discussed in section 4.3.2 only image is required for an accurate cell count. But taking into account the relative low time and effort to take additional images of the same surface, and the chip to image ratio, four images can be taken of the surface. Figure 5 show the suggested way to take four images for highest surface coverage and simplest method. If one image is enough to get an accurate cell count, four images will not result in lower accuracy and would take into account different cell densities over the chip. This experiment show how to execute and verifies the method.

The images are taken as shown in Figure 5 and can be seen in Figure 23. The images is out of focus in the edges of the chip due to surface tension. The liquid raises on the edges of the chamber resulting in difference in focus. The bottom and top pair of images overlap with about 500 pixels. This is in line with Figure 5 and should not impact the result. The images has low quality but are still interesting to analyze because they show the results in an un-optimized setting.

The upper left image in Figure 23 was cropped to 200x200 pixel image in the lower right corner for optimal focus. The cropped image was manually counted and automatically analyzed with the “Dminanalyzer” pipeline. The result can be seen in Figure 24. The D_{min} was set to 3 pixels because it was closest the manually counted number. The manually counted is very similar to the automatically counted which can be seen in Figure 24. The image is not optimal and cells has heterogeneous illumination which makes manually and counting difficult. When

"DminAnalyzer" pipeline processed the whole image the curve has the same shape as the 200x200 pixel cropped image as can be seen in Figure 26 and Figure 25. This indicates that the 200x200 cropped image is representative of the whole image.

All four images was then analyzed with the "CellCount" pipeline with the D_{min} set to 3. The nuclei identified can be seen in Figure 25. Around the edges of the images, where the image is out of focus, cells are not counted. This can be seen as black areas in the outside edges of the images indicating that no nuclei has been detected in that area. This could be solved by remove or fill up all of the liquid in the chips chamber. Another possibility is to cut the image by around 200px on the edges and recalculate the cell number and image area. This will not take into account the difference in cell density that can be seen around the edges of the images.

The results from the "CellCount" pipeline can be seen in Table 11. The "CellCount" pipeline analyses the image two times. The first time it takes into account the object that touches the border of the image. The second time it discards objects touching the sides. This make sure that the objects counted is whole objects and not half object. The script "CellCountCompiler" summaries the number from all four images and all eight analyzations. The resulting mean value seen in Table 11 is the number used for estimating the cell count for the whole chip. In this case, as stated previously, it is not precise because part of the image is out of focus. If the image would be as clear as the images in Figure 18, a more accurate cell count could be achieved. Nevertheless, it show proof of concept that this method is labor free and accurate.

4.3.4 Data compilation script

The script "CellCountCompiler" was written in Python using PyCharm as an IDE and can be seen in Appendix 1. The script extracts the number of nuclei identified in each analyzation. Then it calculates the average for the whole set and prints the result. The script also extracts the area covered by objects that can be used to calculate the confluence on an image if membrane is stained. After installation of necessary programs the script is very user friendly. The only thing that users need to change is the the_path variable in line 7 in Appendix 1. The script is therefore easy to share with customers or calculate in-house. The data can also be extracted manually but takes more time when you have several analyzations in one pipeline and several images processed at once. The scripts purpose is to facilitate easy data extraction use of the pipelines output.

4.3.5 Analyzing the shape of "DminAnalyzer" data curve

When looking at all the plot of the data from the "DminAnalyzer" pipeline a pattern emerges. There is a sharp slope to around where D_{min} is equal to three. Then the slope levels out and derivate is low. Then around D_{min} equal to seven the slope increases again. All of the curves has this general shape of high derivate, low derivate and high derivate. This indicates that the number of cells counted doesn't change significantly in the area with low derivate. In Table 9 there is a parameter called "10^{th} percentile" that shows the diameter counted has that diameter or lower diameter. This is number is 9.1 and 10 per cent of the objects are between 4 and 9.1 in diameter. If the D_{min} is wrong by 1 or 2 pixel in section with low derivate it will not affect the result significantly.

5 Conclusion

5.1 SCK

A high throughput SCK protocol has been developed for Attana's QCM biosensors. This method is faster and can handle a wider range of interactions than the standard methodology. Due to a lack of time, the method is not fully statistically validated, but I am confident that it can be achieved with relative low effort because the interaction has now been fully optimized. This method has great potential to be the standard method for kinetic evaluation at Attana.

5.2 Nanoparticles

The SCK protocol has been tested on nanoparticles. The experiment has shown that SCK methodology can be applied on nanoparticle epitope characterization and further experimental optimization is needed. The method is more than 3 times faster than standard methods and can handle a wider range of interactions. The methodology has great potential to become a standard method for nanoparticle epitope characterization.

5.3 Cell counting

Image analysis is a valuable tool to have for extraction of data. The experiments has shown that accurate cell count can be achieved with relative low effort. The data extracted can be very valuable and improves Attana's cell based assay. Further research should look into determine a standard method to determine confluence. This would include staining of both nuclei and membrane and addition of one module in the "CellCount" pipeline. This report have shown the power of automatic image analyzation which can both save time and money for Attana.

6 Future work

- Complete the myoglobin anti-myoglobin interaction with both methods on the same machine in triplicates. Due to complications with the machine, replication of the experiment was not completed in triplicates. When the problem with the machine has been addressed repeat the experiment described in section 2.1.1 one more time and perform statistical analysis on the resulting data set described in 2.1.2.2.

- Perform an additional SCK biochemical interaction with higher dissociation rate. This will show that SCK experiment can handle a broad range of interaction. This would be a good addition to a future publication.

- Test the SCK statistical variability between machines. In this report the variability on the same machine. By testing on different machines one can determine if the same result can be achieved as MCK on different machines.

- Perform a SCK cell based experiment. This will show that SCK experiment can work on cell based assays. This is very sought after and should be done due to the time save It can achieve. The SCK should be tested on a known system for optimal experimental planning.

- Publishing these results in a method journal. This would without doubt determine the possibility to perform SCK experiment on Attana's biosensors. It would also be a good advertisement for Attana and a source to site when talking to customers

- Perform SCK on 200 nm transferrin coted polystyrene nanoparticle. This would determine the anti-transferrin antibody binding epitopes on nanoparticle corona.

- Program automated concentration determination software. Because SCK experiments are concentration sensitive, automated program to determine the optimal concentrations could be useful. This would decrease the time to plan an experiment and lower the education level needed to operate a biosensor.

- To be able to more accurate determine if the cell counting is accurate several different chips need to analyzed. This will also make possible to statistical determine the error using the cell counting method described in this report.

7 References

[1] I. Brigger, C. Dubernet, och P. Couvreur, ”Nanoparticles in cancer therapy and diagnosis”, *Advanced Drug Delivery Reviews*, vol. 64, Supplement, s. 24–36, dec. 2012.

[2] A. E. Nel, L. Mädler, D. Velegol, T. Xia, E. M. Hoek, P. Somasundaran, F. Klaessig, V. Castranova, och M. Thompson, ”Understanding biophysicochemical interactions at the nano–bio interface”, *Nature materials*, vol. 8, nr 7, s. 543–557, 2009.

[3] S. A. Love, M. A. Maurer-Jones, J. W. Thompson, Y.-S. Lin, och C. L. Haynes, ”Assessing Nanoparticle Toxicity”, *Annual Review of Analytical Chemistry*, vol. 5, nr 1, s. 181–205, 2012.

[4] ”European Commission : CORDIS : Projects & Results Service : NanoClassifier - QCM for rapid label-free Bionano interface evaluation and screening of effectiveness of nano-targeting strategies for therapeutics”. [Online]. http://cordis.europa.eu/project/rcn/111260_en.html. [Accessed: 27-maj-2016].

[5] Biacore Assay Handbook. GE-Healthcare, 2012.

[6] M. Lundqvist, J. Stigler, G. Elia, I. Lynch, T. Cedervall, och K. A. Dawson, ”Nanoparticle size and surface properties determine the protein corona with possible implications for biological impacts”, *Proceedings of the National Academy of Sciences*, vol. 105, nr 38, s. 14265–14270, 2008.

[7] S. Milani, F. Baldelli Bombelli, A. S. Pitek, K. A. Dawson, och J. Rädler, ”Reversible versus irreversible binding of transferrin to polystyrene nanoparticles: soft and hard corona”, *ACS nano*, vol. 6, nr 3, s. 2532–2541, 2012.

[8] P. M. Kelly, C. Åberg, E. Polo, A. O’Connell, J. Cookman, J. Fallon, Ž. Krpetić, och K. A. Dawson, ”Mapping protein binding sites on the biomolecular corona of nanoparticles”, *Nature Nanotechnology*, vol. 10, nr 5, s. 472–479, mar. 2015.

[9] Y. Cheng, O. Zak, P. Aisen, S. C. Harrison, och T. Walz, ”Structure of the Human Transferrin Receptor-Transferrin Complex”, *Cell*, vol. 116, nr 4, s. 565–576, feb. 2004.

[10] D. Zhang, H.-F. Lee, S. C. Pettit, J. L. Zaro, N. Huang, och W.-C. Shen, ”Characterization of transferrin receptor-mediated endocytosis and cellular iron delivery of recombinant human serum transferrin from rice (Oryza sativa L.)”, *BMC Biotechnology*, vol. 12, nr 1, s. 92, 2012.

[12] R. Karlsson, P. S. Katsamba, H. Nordin, E. Pol, och D. G. Myszka, ”Analyzing a kinetic titration series using affinity biosensors”, *Analytical Biochemistry*, vol. 349, nr 1, s. 136–147, feb. 2006.

[13] W. Palau och C. Di Primo, ”Simulated single-cycle kinetics improves the design of surface plasmon resonance assays”, *Talanta*, vol. 114, s. 211–216, sep. 2013.

[14] G. A. Ordway och D. J. Garry, ”Myoglobin: an essential hemoprotein in striated muscle”, *The Journal of experimental biology*, vol. 207, nr Pt 20, s. 3441–3446, sep. 2004.

[15] A. E. Carpenter, T. R. Jones, M. R. Lamprecht, C. Clarke, I. Kang, O. Friman, D. A. Guertin, J. Chang, R. A. Lindquist, J. Moffat, P. Golland, och D. M. Sabatini, ”CellProfiler: image analysis software for identifying and quantifying cell phenotypes”, *Genome Biology*, vol. 7, s. R100, 2006.

[16] K. Tsougeni, G. Papadakis, M. Gianneli, A. Grammoustianou, V. Constantoudis, B. Dupuy, P. S. Petrou, S. E. Kakabakos, A. Tserepi, E. Gizeli, och E. Gogolides, ”Plasma nanotextured polymeric lab-on-a-chip for highly efficient bacteria capture and lysis”, *Lab Chip*, vol. 16, nr 1, s. 120–131, 2016.

[17] M. S. Vokes and A. E. Carpenter, ”Using CellProfiler for Automatic Identification and Measurement of Biological Objects in Images”, *Current Protocols in Molecular Biology*, Red. Hoboken, NJ, USA: John Wiley & Sons, Inc., 2008.

8 Appendix

8.1 Appendix 1

```
import os
import glob
import re

b = []
picture = 0
the_path = r'C:\Users\License\Google Drive\Nanoprojekt\Cellprofiler\results'
for filename in glob.glob(os.path.join(the_path, '*cell*')):  # open all files in the folder contining the line "cell", one at the time
    with open(filename, 'r') as f:                  # open files and read them
        lines = f.readlines()                       # read all the lines in the file
        last_line = lines[lines.__len__()-1].split()        # takes the last line and splits it
        number_of_pictures = int(last_line[0])              # takes the first row number
        # make a list of list in the number of pictures you have
        list_of_pictures = [[] for x in range(number_of_pictures)]  # list for all pictures
        for line in lines:                          # takes one line at the time
            numbers = line.split()          # splits the line at the \t making a list of numbers
            if bool(re.search(r'\d', numbers[1])):      #checking if the first characters is number
                list_of_pictures[int(numbers[0])-1].append(int(numbers[1])) # put in all the numbers in right list
        for picture in list_of_pictures:
            b.append(max(picture))              # takes the max value from all the pictures
    f.close()

result = sum(b)/b.__len__()                 # calculates the mean of the picture objects number

print(b)                                # prints the results
print(result)

# extracts data from the "MyExpt_Experiment"
approx_number = []
myexpt_experiment = os.path.join(the_path,'MyExpt_Experiment.txt')  # locates the experiment file
with open(myexpt_experiment,'r') as f:                  # opens the experiment file
    lines = f.readlines()                               # reads the lines in experiment
    for line in lines:                                  # goes through each line
        if 'Approximate' in line:                       # searches for the line with the word "Approximate"
            area = re.findall('\d+\.\d+', line)             # finds the number describing area in the line
            approx_number.append(area)                      # append the number to a list
        # extract more data add "if" statement here
f.close()                                           # closes the file
area_sum = []
for number in approx_number:                            # summarizes the list
    area_sum.append(number[0])
x = 0
for number in area_sum:
    x += float(number)
the_area = x / area_sum.__len__()                       # calculate the mean area
print(area_sum)
print(the_area)                                     # prints the mean area
```

8.2 Appendix 2

Calculations of mass of nanoparticles. This equation shows how to calculate the density of the combined nanoparticle and transferrin corona. These equation is taken from the supplemental information of article[8] .

$$D_{app}^2 = \frac{D_{PS}^3\rho_{PS} + \left(D_{Ps+Tf}^3 - D_{PS}^3\right)\rho_{Tf} - D_{Ps+Tf}^3\rho_f}{D_{PS+Tf}(\rho_{PS+tf}^3 + \rho_{PS}^3)} \quad \text{(Equation 1)}$$

Equation to calculate the density of transferrin:

$$\rho_{Tf} = \frac{D_{app}^2 D_{PS+Tf}\left(\rho_{PS}^3 + \rho_{Tf}^3\right) - D_{PS}^3\rho_{PS} + D_{Ps+Tf}^3\rho_f}{\left(D_{Ps+Tf}^3 - D_{Ps}^3\right)} \quad \text{(Equation 2)}$$

Variables:

$D_{app} = 141 * 10^{-9}\, m$
$D_{PS100} = 100 * 10^{-9}\, m$
$D_{PS100+Tf} = 108 * 10^{-9}\, m$
$\rho_{PS} = 1.0545 \frac{g}{mol}$
$\rho_f = 1$

$$\rho_{Tf} = \frac{(141 * 10^{-9})^2 * 108 * 10^{-9} * ((100 * 10^{-9})^3 + (108 * 10^{-9})^3) - (100 * 10^{-9})^3 1.0545 + (100 * 10^{-9})^3 1}{(108 * 10^{-9})^3 - (100 * 10^{-9})^3}$$

$\rho_{Tf} = 1.24 \frac{g}{mol}$

Calculating the effective mass (m_{eff}) of NP100@Tf:

$$\frac{m_{eff}}{D_H} = \frac{\frac{\pi}{6} * \left(D_{PS}^3\rho_{PS} + \left(D_{Ps+Tf}^3 - D_{PS}^3\right)\rho_{Tf} - D_{Ps+Tf}^3\rho_f\right)}{D_{PS+Tf}} \quad \text{(Equation 3)}$$

$D_H = 121 * 10^{-9}\, m$
$D_{PS100} = 100 * 10^{-9}\, m$

$D_{PS100+Tf} = 108 * 10^{-9}\, m$

$\rho_{PS} = 1.0545 \frac{g}{ml} = 1.0545 * 10^{6} \frac{g}{m^3}$

$\rho_f = 1 * 10^{6} \frac{g}{m^3}$

$\rho_{Tf} = 1.24 \frac{g}{ml} = 1.24 * 10^{6} \frac{g}{m^3}$

Put in everything in equation 4 and the result is:

$$m_{eff} = \frac{\frac{\pi}{6} * ((100 * 10^{-9})^3 * 1.0545 * 10^6 + ((108 * 10^{-9})^3 - (100 * 10^{-9})^3) * 1.24 * 10^6) - (108 * 10^{-9})^3 * 1 * 10^6) * 121 * 10^{-9}}{100 * 10^{-9}}$$

$$m_{effNP100@Tf} = 6.85 * 10^{-17} g = 6.85 * 10^{-8}\, ng$$

Number of nanoparticles immobilized on chip surface:

$Hertz\ mass\ ration = 0.7 \frac{ng}{Hz}$

$immobilized\ NP100@Tf$: 19 Hz From Figure 16

$N_{NP100@Tf} = \frac{19 * 0.7}{6.85 * 10^{-8}} = 1.94 * 10^8\ st\ NP100@Tf$

Number of antibodies attached to NP100@Tf:

$immobilized\ anti-transferrin$: 1.935 Hz B_{max} from Table 8

$Antibody\ mass$: 150 kDa

$N_{ab\_769} = \frac{1.935 * 0.7 * 10^{-9}}{150\ 000} * 6.022 * 10^{23} = 5.44 * 10^9\ st\ ab\_769$

Number of antibodies per NP100@Tf:

$\frac{N_{ab\_769}}{N_{NP100@Tf}} = \frac{5.44 * 10^9}{1.94 * 10^8} = 28\ ab_{769} per\ NP100@Tf$

Calculating reference

Number of nanoparticles immobilized on chip surface:

$Hertz\ mass\ ration = \ 0.7 \frac{ng}{Hz}$

$immobilized\ NP100@Tf$: 18 Hz

$N_{NP100@Tf} = \frac{18\ * 0.7}{6.85 * 10^{-8}} = 1.84 * 10^{8}\ st\ NP100@Tf$

Number of antibodies attached to NP100@Tf:

$immobilized\ anti - transferrin$: 4,07224 Hz B_{max} from Table 1

$Antibody\ mass$: 150 kDa

$N_{ab\_769} = \frac{4.07224\ * 0.7 * 10^{-9}}{150\ 000} *\ 6.022 * 10^{23} = 1.144 * 10^{10}\ st\ ab\_769$

Number of antibodies per NP100@Tf:

$\frac{N_{ab\_769}}{N_{NP100@Tf}} = \frac{1.144 * 10^{10}}{1.84 * 10^{8}} = 62.17 = 62\ ab_{769}\ per\ NP100@Tf$

8.3 Appendix 3

Creator: Fredrik Boström
Created: 2016-03/22
Comment:
2 1 0.5 0.25 0.125 conc regeneration
ass 84 diss 300
MCK run
SCK run

Row no	Action	Parameter(s)						
1	Flow_Rate	25						
2	Temperature	22						
3	C-Fast_Prime							
4	**SCK**							
5	*Inject_From_MTP1*	*Other*	*AB*	*BLANK*		*35.0*	*300*	*F6*
6	*Inject_From_MTP1*	*Analyte*	*AB*	*myoglobin*	*0.125*	*35.0*	*0*	*F1*
7	*Clean_Loops_From_Wash*	*3*						
8	*Inject_From_MTP1*	*Analyte*	*AB*	*myoglobin*	*0.25*	*35.0*	*0*	*F2*
9	*Clean_Loops_From_Wash*	*3*						
10	*Inject_From_MTP1*	*Analyte*	*AB*	*myoglobin*	*0.5*	*35.0*	*0*	*F3*
11	*Clean_Loops_From_Wash*	*3*						
12	*Inject_From_MTP1*	*Analyte*	*AB*	*myoglobin*	*1*	*35.0*	*0*	*F4*
13	*Clean_Loops_From_Wash*	*3*						
14	*Inject_From_MTP1*	*Analyte*	*AB*	*myoglobin*	*2*	*35.0*	*600*	*F5*
15	*Clean_Loops_From_Wash*	*3*						
16	*Inject_From_Solvent_Tray*	*Regeneration*	*AB*	*GLY*	*0*	*10.0*	*0*	*1*
17	*Wait*	*600*						
18	*Clean_Loops_From_Wash*	*3*						
19	**MCK**							
20	*Inject_From_MTP1*	*Other*	*AB*	*BLANK*	*0*	*35.0*	*300*	*H1*
21	*Inject_From_MTP1*	*Analyte*	*AB*	*myoglobin*	*0.125*	*35.0*	*300*	*G1*
22	*Clean_Loops_From_Wash*	*3*						
23	*Inject_From_Solvent_Tray*	*Regeneration*	*AB*	*GLY*	*0*	*10.0*	*0*	*1*
24	*Wait*	*600*						
25	*Clean_Loops_From_Wash*	*3*						
26	*Inject_From_MTP1*	*Other*	*AB*	*BLANK*	*0*	*35.0*	*300*	*H2*
27	*Inject_From_MTP1*	*Analyte*	*AB*	*myoglobin*	*0.25*	*35.0*	*300*	*G2*
28	*Clean_Loops_From_Wash*	*3*						
29	*Inject_From_Solvent_Tray*	*Regeneration*	*AB*	*GLY*	*0*	*10.0*	*0*	*1*
30	*Wait*	*600*						
31	*Clean_Loops_From_Wash*	*3*						
32	*Inject_From_MTP1*	*Other*	*AB*	*BLANK*	*0*	*35.0*	*300*	*H3*

33	*Inject_From_MTP1*	*Analyte*	*AB*	*myoglobin*	*0.5*	*35.0*	*300*	*G3*
34	*Clean_Loops_From_Wash*	*3*						
35	*Inject_From_Solvent_Tray*	*Regeneration*	*AB*	*GLY*	*0*	*10.0*	*0*	*1*
36	*Wait*	*600*						
37	*Clean_Loops_From_Wash*	*3*						
38	*Inject_From_MTP1*	*Other*	*AB*	*BLANK*	*0*	*35.0*	*300*	*H4*
39	*Inject_From_MTP1*	*Analyte*	*AB*	*myoglobin*	*1*	*35.0*	*300*	*G4*
40	*Clean_Loops_From_Wash*	*3*						
41	*Inject_From_Solvent_Tray*	*Regeneration*	*AB*	*GLY*	*0*	*10.0*	*0*	*1*
42	*Wait*	*600*						
43	*Clean_Loops_From_Wash*	*3*						
44	*Inject_From_MTP1*	*Other*	*AB*	*BLANK*	*0*	*35.0*	*300*	*H5*
45	*Inject_From_MTP1*	*Analyte*	*AB*	*myoglobin*	*2*	*35.0*	*300*	*G5*
46	*Clean_Loops_From_Wash*	*3*						
47	*Inject_From_Solvent_Tray*	*Regeneration*	*AB*	*GLY*	*0*	*10.0*	*0*	*1*
48	*Wait*	*600*						
49	*Clean_Loops_From_Wash*	*3*						
50								
51								

8.4 Appendix 4

List name: NPXXX@Tf - SCK.lst
Creator: NPXXX@Tf SCK and preconditioning
Created:
Comment: general SCK experimental setup for epitope determination

Row no	Action	Parameter(s)						
1	Flow_Rate	25						
2	Temperature	22						
3	C-Fast_Prime							
4	**SCK NP200@Tf**							
5	*Inject_From_MTP1*	*Reference*	*AB*	*BLANK*	*0*	*35.0*	*300*	*A1*
6	*Inject_From_MTP1*	*Ligand*	*AB*	*NPXXXTf*	*40*	*35.0*	*300*	*B1*
7	*Flow_Rate*	*10*						
8	*Wait*	*300*						
9	*Clean_Loops_From_Wash*	*3*						
10	*Inject_From_MTP1*	*Reference*	*AB*	*BLANK*	*0*	*35.0*	*300*	*A1*
11	*Inject_From_MTP1*	*Analyte*	*AB*	*ab_769*	*1.25*	*35.0*	*210*	*A2*
12	*Clean_Loops_From_Wash*	*3*						
13	*Inject_From_MTP1*	*Analyte*	*AB*	*ab_769*	*2.5*	*35.0*	*210*	*A3*
14	*Clean_Loops_From_Wash*	*3*						
15	*Inject_From_MTP1*	*Analyte*	*AB*	*ab_769*	*5*	*35.0*	*210*	*A4*
16	*Clean_Loops_From_Wash*	*3*						
17	*Inject_From_MTP1*	*Analyte*	*AB*	*ab_769*	*10*	*35.0*	*210*	*A5*
18	*Clean_Loops_From_Wash*	*3*						
19	*Inject_From_MTP1*	*Analyte*	*AB*	*ab_769*	*20*	*35.0*	*1000*	*A6*
20	*Clean_Loops_From_Wash*	*3*						
21	Inject_From_Solvent_Tray	Regeneration	AB	GLY	0	35.0	0	1
22	Wait	600						
23	Idle	200	99.0	25				
24								